NPS ARCHIVE
1967
LEWIT, H.

THE EXPERIMENTAL MODIFICATION OF A BAROTROPIC NUMERICAL PREDICTION MODEL

HOWARD LEO LEWIT

[redacted]

THE EXPERIMENTAL MODIFICATION OF A BAROTROPIC NUMERICAL PREDICTION MODEL

by

Howard Leo Lewit
Lieutenant Commander, United States Navy
B.S., New York University, 1950
M.A., New York University, 1953

Submitted in partial fulfillment of the
requirements for the degree of

MASTER OF SCIENCE IN METEOROLOGY

from the

NAVAL POSTGRADUATE SCHOOL
June 1967

ABSTRACT

There were two objectives in the experiments performed on the barotropic model. One was to correct the lag of the troughs and ridges noted in the barotropic model by the Naval Weather Research Facility, and the other was to introduce a baroclinic development term.

The approach to these problems was one which could be incorporated into the Fleet Numerical Weather Facility model with ease.

Included herein are the theoretical development of the numerical model, a comparison with the FNWF model and charts illustrative of the results with various values of the pertinent parameters for 24 and 48 hours.

It was observed that the development term causes selective development of lows and highs; but when overdone, spurious short waves are formed which, however, do not basically change the major wave location.

It was also observed that the function of latitude used here to correct the lag in the horizontal advection of vorticity, resulted in greatly improved movement of troughs and ridges from 30 degrees to 60 degrees of latitude, but could be further refined to produce even better results.

LIBRARY
NAVAL POSTGRADUATE SCHOOL
MONTEREY, CALIF. 93940

TABLE OF CONTENTS

Section		Page
1.	Introduction	11
2.	The FNWF model	12
3.	The baroclinic model	14
4.	The numerical form of the baroclinic equation	17
5.	Research Procedure	19
6.	Experimental Results	21
7.	Independent data test	54
8.	Conclusions	57
9.	Acknowledgment	59
10.	Bibliography	60

LIST OF TABLES

Table		Page
1.	24-Hour prognostic displacement of troughs and ridges from analysis with and without latitude function.	25
2.	Pillow and RMSE of independent data, with and without latitude function, and FNWF.	26
3.	Comparative results of varied development term vice smoothing	52
4.	Independent data test of development term	55
5.	Pillow and RMSE of independent data, varied development term and FNWF.	56

LIST OF ILLUSTRATIONS

Figure		Page
1.	Sine Latitude function	22
2.	24-hour prognostic chart verifying time (V. T.) 0000Z 26 Jan 1967, no sine latitude function.	23
3.	24-hour prognostic chart V. T. 0000Z 26 Jan 1967, with sine latitude function.	24
4.	0000Z 25 Jan 1967 500-mb analysis	28
5.	0000Z 26 Jan 1967 500-mb analysis	29
6.	24-hour prognostic chart V. T. 0000Z 26 Jan 1967, no development term.	31
7.	24-hour prognostic chart V. T. 0000Z 26 Jan 1967, 0.5 of development term.	33
8.	24-hour prognostic chart V. T. 0000Z 26 Jan 1967, 1.0 of development term.	34
9.	24-hour prognostic chart V. T. 0000Z 26 Jan 1967, no development term with heavy smoother.	36
10.	24-hour prognostic chart V. T. 0000Z 26 Jan 1967, 1.0 of development term with heavy smoother.	37
11.	24-hour prognostic chart V. T. 0000Z 26 Jan 1967, 1.0 of development term with no periodic reduction, heavy smoother.	39
12.	24-hour prognostic chart V. T. 0000Z 26 Jan 1967, 2.0 of development term.	40
13.	24-hour prognostic chart V. T. 0000Z 26 Jan 1967, 1.0 of development term, 1/2 of heavy smoother.	41
14.	24-hour prognostic chart V. T. 0000Z 26 Jan 1967, 1.0 of development term, 1/4 of heavy smoother.	43
15.	1200Z 25 Jan 1967 500-mb analysis	44

Figure Page

16. 48-hour prognostic chart V.T. 1200Z 25 Jan 1967, no development term with heavy smoother. 45

17. 48-hour prognostic chart V.T. 1200Z 25 Jan 1967, 1.0 of development term, heavy smoother. 46

18. 48-hour prognostic chart V.T. 1200Z 25 Jan 1967, no development term 1/2 of heavy smoother. 48

19. 48-hour prognostic chart V.T. 1200Z 25 Jan 1967, 1.0 of development term, 1/2 of heavy smoother. 49

20. 48-hour prognostic chart V.T. 1200Z 25 Jan 1967, 1.0 of development term, 1/2 of heavy smoother twice every 6 hours vice three times. 50

TABLE OF SYMBOLS AND ABBREVIATIONS

mb	Millibars
FNWF	Fleet Numerical Weather Facility, Monterey, Cal.
f	Coriolis parameter
$\mathcal{S}$	Relative vorticity
$\mathcal{Z}$	Absolute vorticity
h, H	Thickness
$\mathbb{W}$	Horizontal wind velocity
$\mathbb{W}_T$	Horizontal thermal wind velocity
$\mathcal{S}_T$	Relative thermal vorticity
Z	Height
g	Acceleration of gravity
D	Height less standard height
^	A scaled parameter
m	Map factor
d	Distance between grid points
K_2	advection of horizontal vorticity tuning constant
K_3	development term tuning constant
k	smoothing factor
ϕ	Latitude

1. Introduction

The numerical model for the prognosis of the 500-mb level used by the FNWF is based upon the barotropic potential vorticity equation [3]. This model has been carefully "tuned" and engineered over a period of several years and is found to produce quite satisfactory results. The use of a numerical model derived from a baroclinic vorticity equation, however, should improve prognosis by permitting development and decay of pressure systems. Due to time limitations, it was decided to utilize a quasi-baroclinic model which makes use of of the initial (1000-500)-mb thickness and a simplified prognosis thereof to compute a Sutcliffe development term in the 500-mb prognostic equation. No attempt is made to verify the thickness forecasts nor the implied 1000-mb prognosis.

The model developed and tested here is still essentially a one-parameter model and constitutes only an attemp to provide for some development in the conventional barotropic model, which is the primary shortcoming of an otherwise very successful prediction scheme for mid-troposphere.

In addition to the use of a baroclinic term, some experimentation was performed on the horizontal vorticity advection term of the equation by varying it as a function of latitude. Various degrees of smoothing were also applied to the prognosis and the effects on the appearance and verification are noted.

2. The FNWF model [3]

The barotropic potential vorticity equation is taken as

$$\frac{D}{Dt}\left(\frac{f+\mathcal{J}}{h}\right)=0 \tag{2.1}$$

where h is the depth of fluid being considered. For application to the atmosphere, this layer is considered to be approximately the troposphere and to be centered at the 500-mb level. Expanding equation 2.1 and multiplying through by h gives

$$\frac{\partial(f+\mathcal{J})}{\partial t}-\frac{1}{h}(f+\mathcal{J})\frac{\partial h}{\partial t}+\mathbf{V}\cdot\nabla f+\mathbf{V}\cdot\nabla\mathcal{J}-\frac{1}{h}(f+\mathcal{J})\mathbf{V}\cdot\nabla h=0 \tag{2.2}$$

The last term is assumed to be composed of three components; namely,

a) a mountain term,

b) a latitude term,

c) a temperature term.

Equation 2.2 then becomes

$$\underset{(1)}{\frac{\partial(f+\mathcal{J})}{\partial t}}\underset{(2)}{-\frac{1}{h}(f+\mathcal{J})\frac{\partial h}{\partial t}}+\underset{(3)}{\mathbf{V}\cdot\nabla f}+\underset{(4)}{\mathbf{V}\cdot\nabla\mathcal{J}}\underset{(5)}{-\frac{1}{h}(f+\mathcal{J})\mathbf{V}\cdot\nabla h_1}\underset{(6)}{-\frac{1}{h}(f+\mathcal{J})\mathbf{V}\cdot\nabla h_2}\underset{(7)}{-\frac{1}{h}(f+\mathcal{J})\mathbf{V}\cdot\nabla h_3}=0 \tag{2.3}$$

Term (2) is the Helmholtz term. It is approximated by

$$\frac{1}{h}(f+\mathcal{J})\frac{\partial h}{\partial t}\approx\frac{\mu}{\bar{h}}\bar{f}\frac{\partial Z}{\partial t}=A\frac{\partial Z}{\partial t} \tag{2.4}$$

where Z is the height of the 500-mb surface, f is a mean value for $(f+\mathcal{J})$, $\bar{h}$ is a mean value for h, and μ is a constant determined by experimentation.

Term (5) is a mountain term. The approximation

$$-\frac{1}{h}(f+\zeta)\mathbf{V}\cdot\nabla h_1 \approx -a\frac{f}{h}\mathbf{V}\cdot\nabla M \approx -\mathbf{V}\cdot\nabla\frac{afM}{\bar{h}} \qquad (2.5)$$

is made where M is the height of the terrain, and "a" is an emperically determined constant. With other considerations and simplifications this results in

$$(\nabla^2 - A)\frac{\partial\chi}{\partial t} = -\mathbf{V}\cdot\nabla\left(f+\zeta+af M - \frac{bf\bar{H}}{\bar{h}}\right) \qquad (2.6)$$

where "b" is a tuning constant and H is a (500-1000)-mb thickness.

The thickness is carried forward during the forecast as an independent field with half of the speed of the 500-mb wind.

In addition to the above, other engineering and climatological modifications are made in the FNWF model but will not be discussed here.

3. The baroclinic model

The baroclinic model used here is developed from the horizontal advective model [2, p. 400] in which temperature changes are assumed to result from horizontal advection only. In this model, it is also assumed that the vertical variation of the magnitude of the thermal wind is the same everywhere and the wind field may be expressed

$$\mathbb{V} = \overline{\mathbb{V}} + A(p)\mathbb{V}_T \tag{3.1}$$

where $\overline{\mathbb{V}}$ is the vertically integrated mean wind with respect to pressure and $\mathbb{V}_T$ is the vector difference between the wind at two selected isobaric levels. With the geostrophic assumption, $\mathbf{V}_T$ is the thermal wind.

By the same assumption

$$\mathcal{T} = \overline{\mathcal{T}} + A(p)\mathcal{T}_T \tag{3.2}$$

Integrating the vorticity equation

$$\frac{\partial \mathcal{T}}{\partial t} + \mathbb{V}\cdot\nabla(f+\mathcal{T}) = \bar{f}\frac{\partial \omega}{\partial p} \tag{3.3}$$

after substituting from (3.1) and (3.2) gives

$$\frac{1}{p_0}\int_0^{p_0}\frac{\partial}{\partial t}(\overline{\mathcal{T}}+A(p)\mathcal{T}_T)\,dp + \frac{1}{p_0}\int_0^{p_0}(\overline{\mathbb{V}}+A(p)\mathbb{V}_T)\cdot\nabla(\overline{\mathcal{T}}+A(p)\mathcal{T}_T+f)\,dp = \bar{f}\,\omega_{1000} \tag{3.4}$$

The left side leads to

$$\frac{\partial \overline{\mathcal{T}}}{\partial t} + \overline{\mathbb{V}}\cdot\nabla_p(\overline{\mathcal{T}}+f) + \overline{A^2}\,\mathbb{V}_T\cdot\nabla_p\mathcal{T} \tag{3.5}$$

By the geostrophic approximation

$$\bar{V} = \frac{g}{f} k \times \nabla \bar{z} \tag{3.6A}$$

$$\bar{\mathcal{J}} = \frac{g}{f} \nabla^2 \bar{z} \tag{3.6B}$$

$$V_T = \frac{g}{f} k \times \nabla H \tag{3.6C}$$

$$\mathcal{J}_T = \frac{g}{f} \nabla^2 H \tag{3.6D}$$

substituting (3.6) into (3.5)

$$\frac{g}{f} \nabla^2 \frac{\partial \bar{z}}{\partial t} + \frac{g}{f} k \times \nabla \bar{z} \cdot \nabla_p (\bar{\mathcal{J}} + f) + \bar{A}^2 \frac{g}{f} k \times \nabla H \cdot \nabla_p \frac{g}{f} \nabla^2 H \tag{3.7}$$

leads to

$$\nabla^2 \frac{\partial \bar{z}}{\partial t} + \left(-\frac{\partial \bar{z}}{\partial y} \frac{\partial}{\partial x} + \frac{\partial \bar{z}}{\partial x} \frac{\partial}{\partial y} \right) + \bar{A}^2 \left(-\frac{\partial H}{\partial y} \frac{\partial \frac{g}{f} \nabla^2 H}{\partial x} + \frac{\partial H}{\partial x} \frac{\partial \frac{g}{f} \nabla^2 H}{\partial y} \right) \tag{3.8}$$

using

$$J(A,B) = \left(\frac{\partial A}{\partial x} \frac{\partial B}{\partial y} - \frac{\partial B}{\partial x} \frac{\partial A}{\partial y} \right)$$

3.8 becomes

$$\nabla^2 \frac{\partial \bar{z}}{\partial t} + J(z, \nabla) + \bar{A}^2 J\left(H, \frac{g}{f} \nabla^2 H\right) \tag{3.9}$$

The right side of (3.4) leads to a Helmholtz term for which the FNWF version is utilized. Introducing tuning coefficients K_2 and K_3 yields to the final operational equation

$$(\nabla^2 - A) \frac{\partial z}{\partial t} = -K_2 J(z, \nabla) - K_3 J\left(H, \frac{g}{f} \nabla^2 H\right) \tag{3.10}$$

where Z is the 500-mb height, H is the (500-1000)-mb thickness, and A is the FNWF Helmholtz term. Assuming the thickness changes are purely advective gives

$$\frac{\partial H}{\partial t} + K_4 \bar{\nabla} \cdot \nabla_p H = 0 \qquad \text{OR} \qquad \frac{\partial H}{\partial t} = -K_4 \frac{g}{f} J(Z, H) \tag{3.11}$$

where K_4 is 0.5.

4. The numerical form of the baroclinic equation

Equations (3.10) and (3.11) are solved over a field composed of 63x63 grid points which are a distance d apart. The appropriate map factor m for the FNWF 63x63 grid is that for a polar stereographic projection [1] . In order to utilize the FNWF subroutine library and reduce computation time, fixed point arithmetic was used. The constants and corresponding scaling factors are:

$d = 381\text{KM} = 3.81 \times 10^{7}$ cm

$m = 2\hat{m}$

$f = 1.03125 \times 10^{-4}$ sec^{-1}

$g = 980$ cm sec^{-2}

$D = \hat{D} \times 2^{17}$ $(D = Z - Z_{std})$

$H = \hat{H} \times 2^{17}$

$\zeta = \hat{\zeta} \times 2^{-9}$

$\mathcal{F}_T = \hat{\mathcal{F}}_T \times 2^{-9}$ $\left(\frac{g}{f}\nabla^2 H = \mathcal{F}_T\right)$

$\Delta t = 1$ hour $= 3600$ secs

which result in

$$(\nabla^2 - A)\Delta\hat{D} = -K_2 \times 2 \times .878 \times J(\hat{D}, \hat{\zeta}) - K_3 \times 2 \times .878 \times J(\hat{H}, \hat{\mathcal{F}}_T) \qquad (4.1)$$

which is the form of equation (3.10) used in the FNWF Helmholtz subroutine [1] .

The thickness is carried forward during the forecast as an independent field with half of the speed of the 500-mb wind

$$\frac{\partial H}{\partial t} = -\frac{1}{2}\mathbf{V}\cdot\nabla H = -\frac{1}{2}J(Z, H) \qquad (4.2)$$

When expressed in finite difference form, (4.2) becomes

$$\Delta \hat{H} = -2 \times .775 \times \hat{m}^2 \times J(\hat{D}, \hat{H}) \tag{4.3}$$

Both (4.1) and (4.3) are computed on an hourly basis. The first time step is produced by the method of forward time differences

$$D^{m+1} = D^m + \Delta D^m \tag{4.4}$$

If continued, this method would lead to computational instability. For this reason, all other time steps are produced by the method of centered time differencing 4

$$D^{m+1} = D^{m-1} + 2\Delta D^m \tag{4.5}$$

In the event a smoothing operation is performed on a field, a forward time difference is used as the subsequent time step.

5. Research procedures

Comparing equations (2. 5) and (3. 10) shows that the FNWF model without certain refinements closely approximates the baroclinic model when K_3 is zero. For this reason, this baroclinic model without the development term can be referred to as the quasi-FNWF model; however, the FNWF model has additional refinements not included here, hence comparisons of verification scores are not strictly valid.

The data used for the experiments were recent 500-mb and (500-1000)-mb thickness fields obtained from FNWF. The actual computing was done on the Postgraduate School Computer Facility CDC Model 1604.

The results of each experimental run were tested by the pillow and RMSE [1], then analyzed and visually compared with the analysis at verification time as well as with other experimental runs.

Pillow $$\frac{\sum_{N=1}^{X} (A-B)_N}{X}$$

RMSE $$\sqrt{\sum_{N=1}^{X} \frac{[(A-B)-\text{Pillow}]^2_N}{X}}$$

It is apparent that the RMSE, although a rapid method of quantitative comparison of fields, will not show a variation of development of systems. It was therefore necessary to use the visual method.

The experimental procedure consisted of varying the values of K_2 or K_3 or both. The values of K_3 varied from 0 to 2.0 and also included variations of the tuning constants with respect to latitude.

In addition to the above, the fields were compared after different degrees of smoothing were applied.

6. Experimental results

Consider first the advection term only. The speed of movement of the troughs and ridges were modified by the use of K_2 as a function of latitude. The need for this modification was made evident by a study of the FNWF model conducted by the Naval Weather Research Facility, Norfolk, Virginia, which indicated consistently slow movement of troughs and ridges through certain latitudes, a deficiency that appears to characterize barotropic models in general and even some baroclinic models.

After several trials, an emperical correction was made for this lag by the employment of a function of latitude (SF) as the factor

$$\frac{.5 + \sin\phi}{.5 + \sin^2\phi}$$

applied to the horizontal vorticity advection,

The graph of this function, Fig. 1, shows a maximum of 1.37 at 21.4 degrees and a value of one at the equator and pole.

The effect of the use of this sine function can be seen by comparing Fig. 2, the 24-hour prognostic chart without the sine function and Fig. 3, in which the sine function is applied.

There is an obvious displacement of all systems while the contour shape remains essentially unchanged.

To test the effectiveness of this function on independent data, a test was run on seven consecutive 24-hour periods from 0000Z 24 March to 0000Z 27 March. The displacement of troughs and ridges was measured in degrees of latitude and an average deviation from the

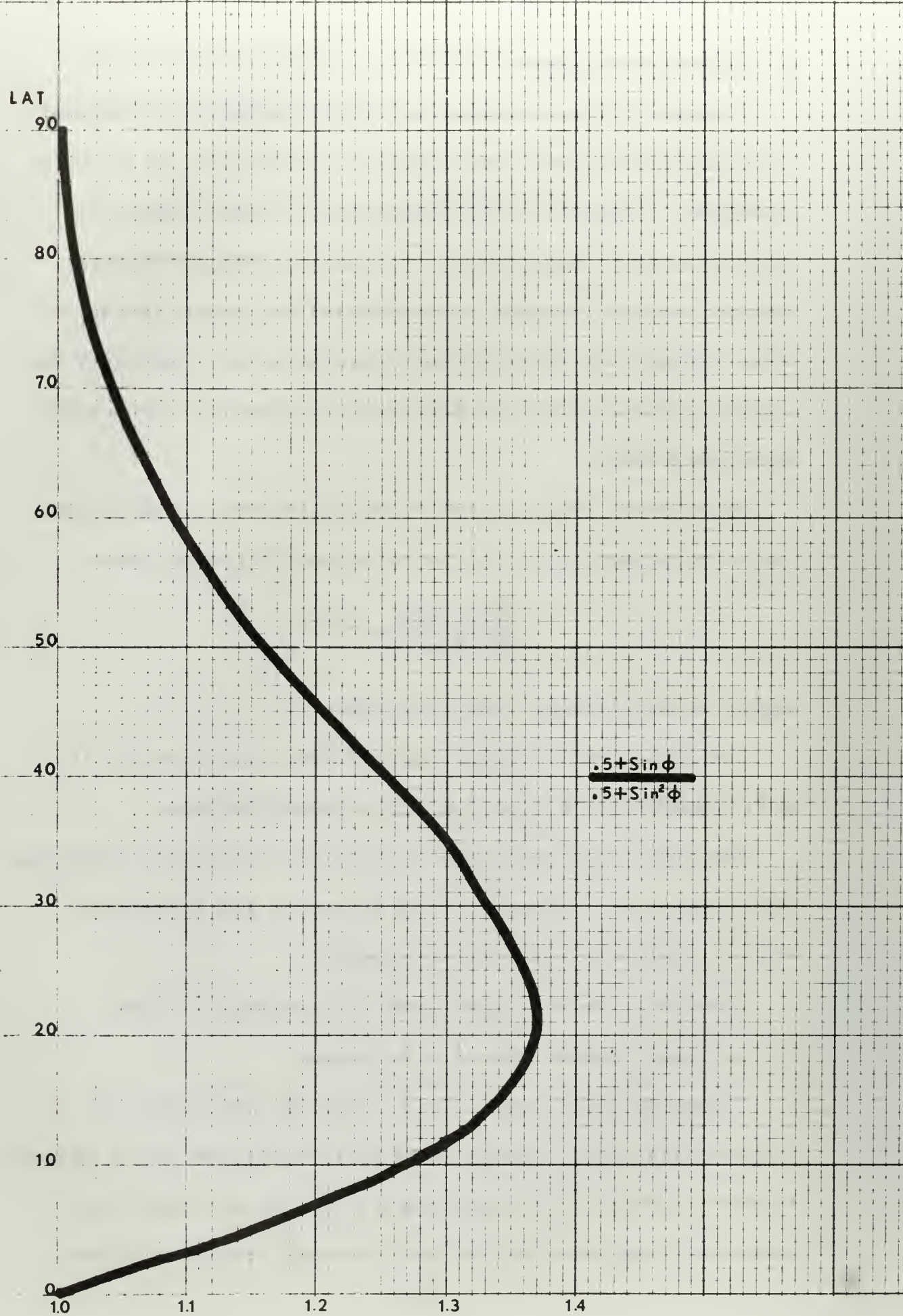


FIG. 1

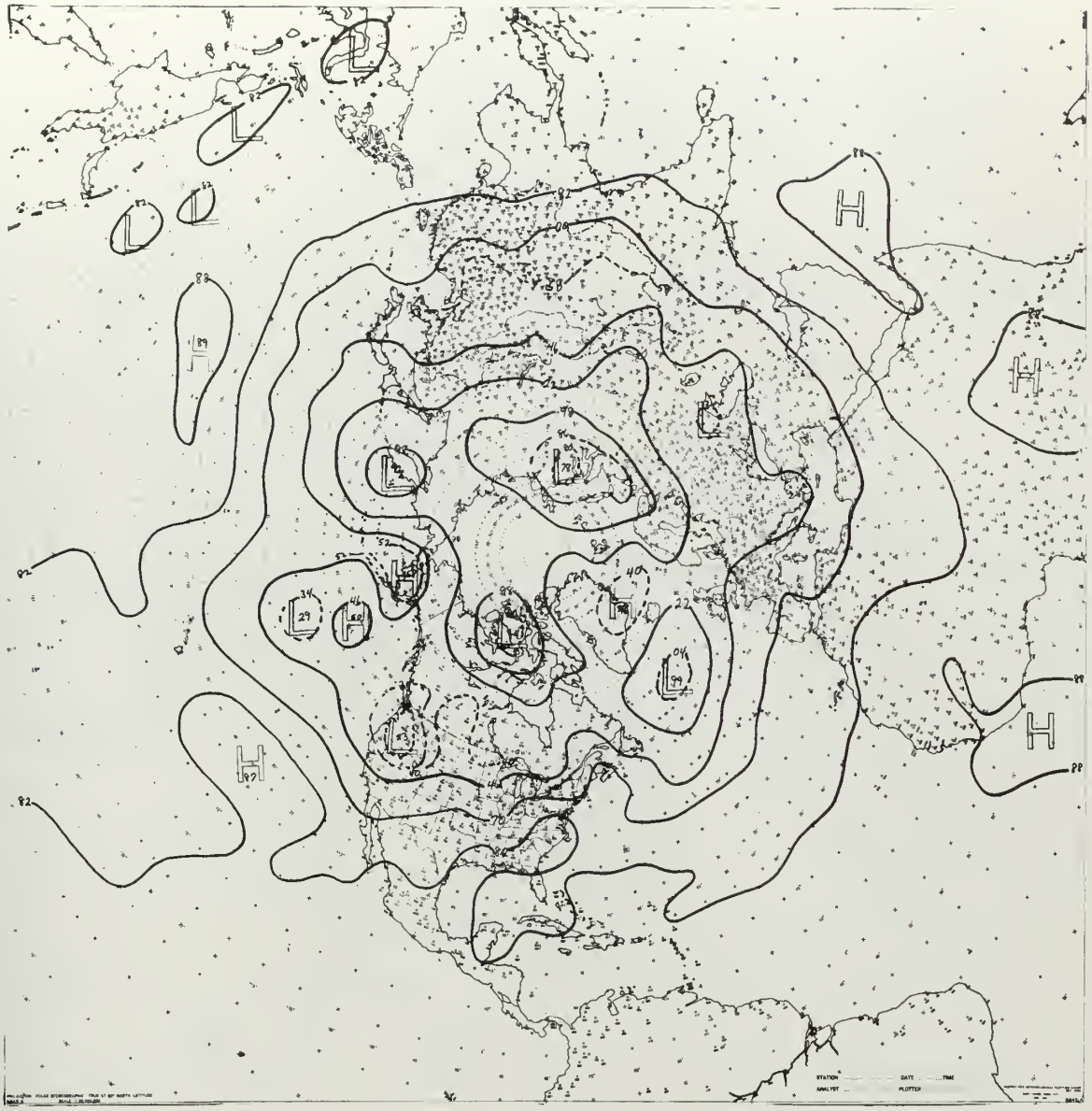


Fig. 2

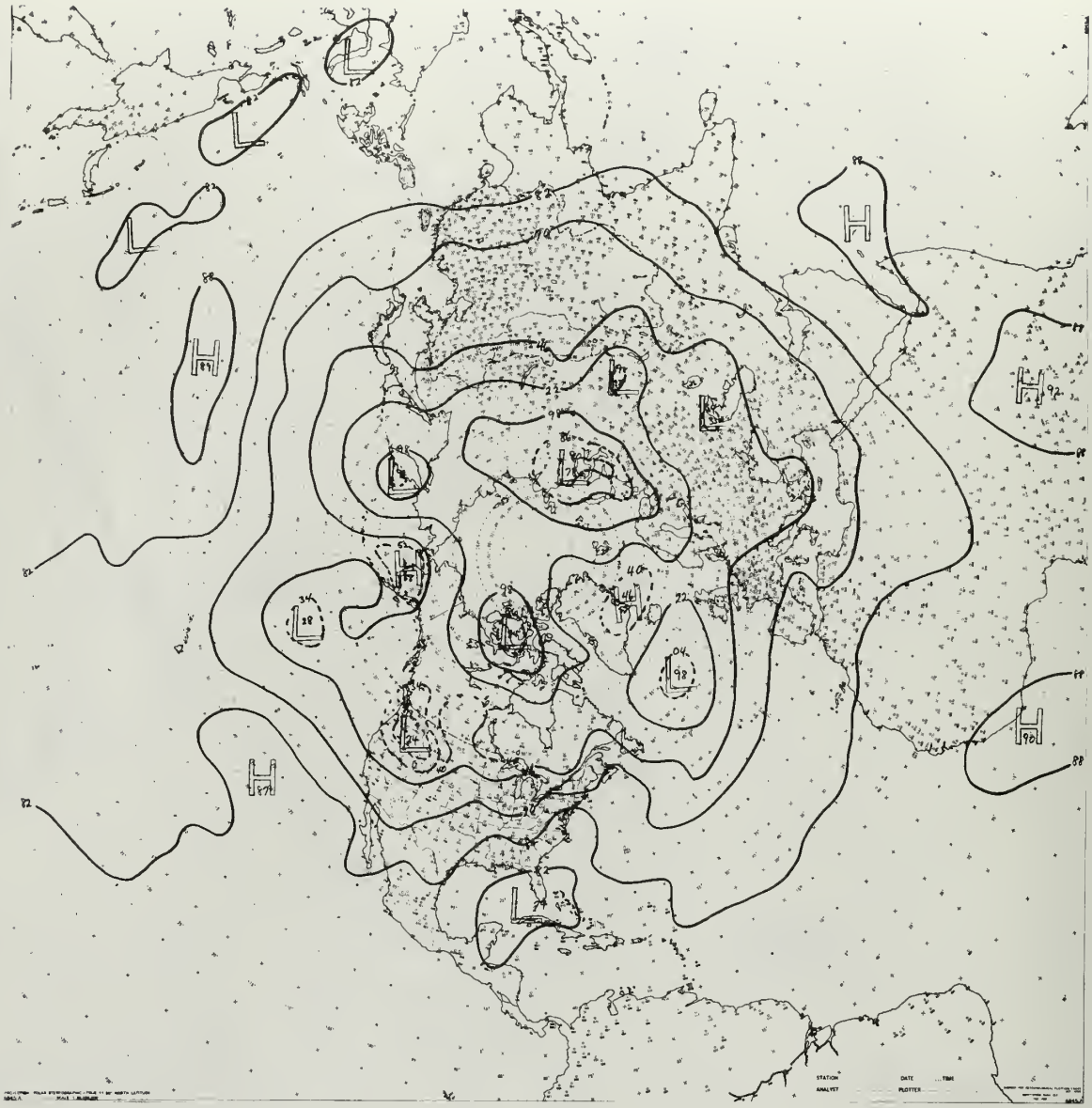


Fig. 3

TABLE I

24-Hr Prog

AVERAGE DISPLACEMENT FROM
ANALYSIS
IN DEGREES OF LATITUDE

LAT	WITH SINE FUNCTION			WITHOUT SINE FUNCTION		
	TROUGHS	RIDGES	COMBINED	TROUGHS	RIDGES	COMBINED
10	-2.72(11)	-2.0(2)	-2.62(13)	-2.64(11)	-2.0(2)	-2.54(13)
20	1.43(23)	-.36(14)	.76(37)	.61(23)	-.93(14)	.03(37)
30	.70(36)	-1.91(23)	-.32(59)	-.97(36)	-2.26(23)	-1.47(59)
40	.51(35)	-2.40(30)	-.83(65)	-.66(35)	-3.57(30)	-2.00(65)
50	-.35(31)	-2.15(26)	-1.16(57)	-1.52(31)	-3.46(26)	-2.40(57)
60	-1.66(18)	-.95(20)	-1.30(38)	-2.38(18)	-2.15(20)	-2.26(38)

(# of samples)

TABLE II

24-Hr Prog

TEST OF SINE FACTOR

PILLOW* RMSE*

V.T.	NO SF		WITH SF		FNWF	
00Z 24 Mar	-1	93	-2	94	1.1	104
12Z 24 Mar	-5	101	-5	102	6.3	115.3
00Z 25 Mar	-5	90	-5	91	6.6	108.3
12Z 25 Mar	5	97	5	97	-3.8	105.9
00Z 26 Mar	0	113	0	113	- .3	111.1
12Z 26 Mar	-2	117	-2	116	-1.2	115.0
00Z 27 Mar	18	94	18	95	-25.5	101.5

*feet

corresponding analysis was taken for the entire period.

The results of this test are summarized in Table I. The first item observed by this summary was that the movement of troughs and ridges was truly in need of an increase at almost all latitudes tabulated. It is seen that the use of the sine function produces a distinct improvement from 30 to 60 degrees. This is particularly evident in the "combined" column which includes troughs and ridges.

Table I also shows a possibility of too much correction at 20 degrees.

The results at 10 degrees are considered to be inconclusive due to the small number of samples and the difficulty of defining troughs at this latitude.

Table II compares the pillow and RMSE for the verification dates of the test without the sine function, with the sine function and for the FNWF product. The use of the sine function produces little change in this statistic.

Turning now to the development of systems, the problem was to define a proper K_3 term or to determine how much development term to use.

The experimental data was selected at random from the FNWF files of height fields and corresponding thickness fields.

The 24-hour prognostic tests were run from 0000Z 25 Jan 1967, Fig. 4, to 0000Z 26 Jan 1967, Fig 5. This date was chosen at random and, although not the best of all possible situations to illustrate development, does show the effects of the several variations.

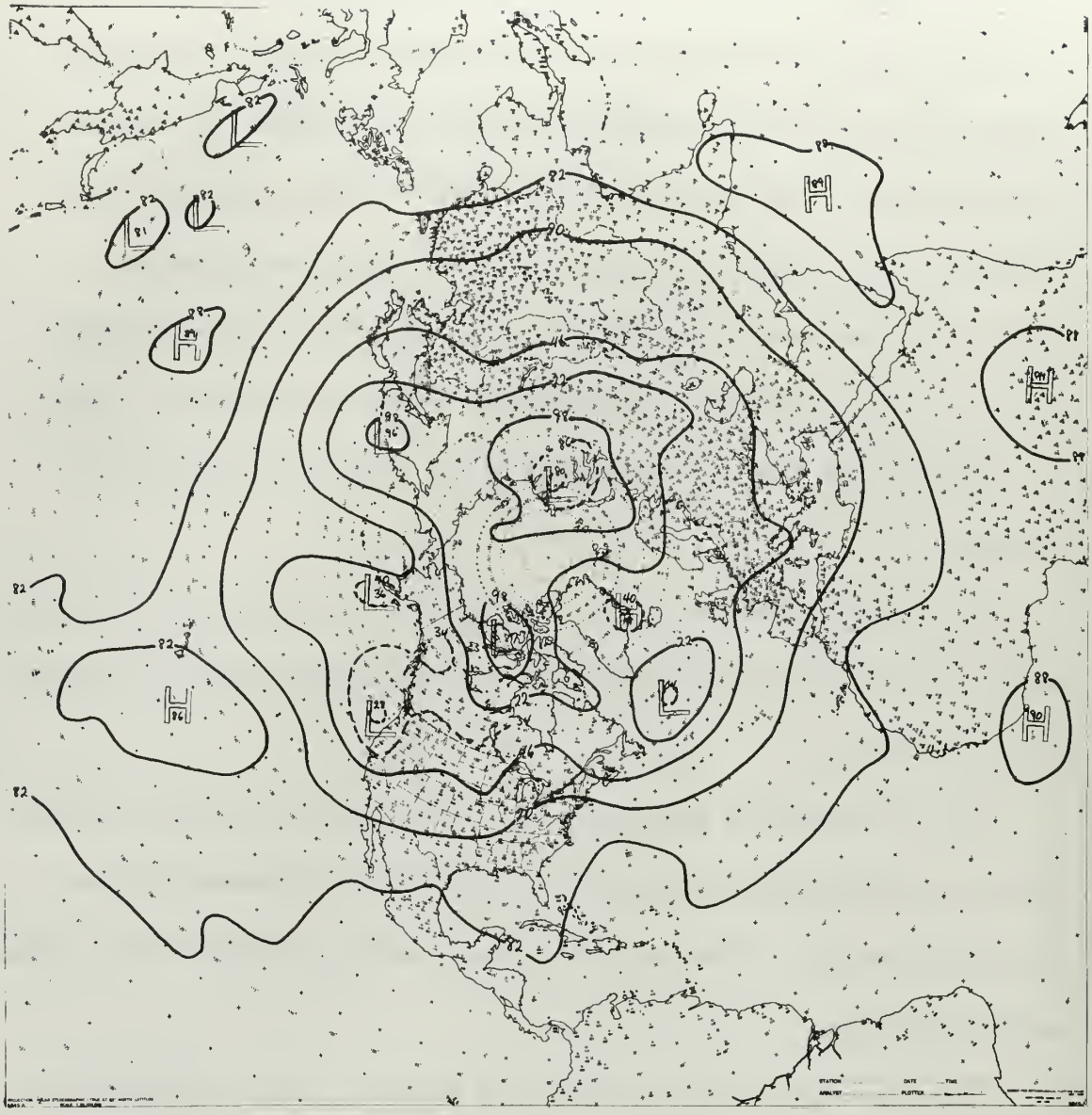


Fig. 4

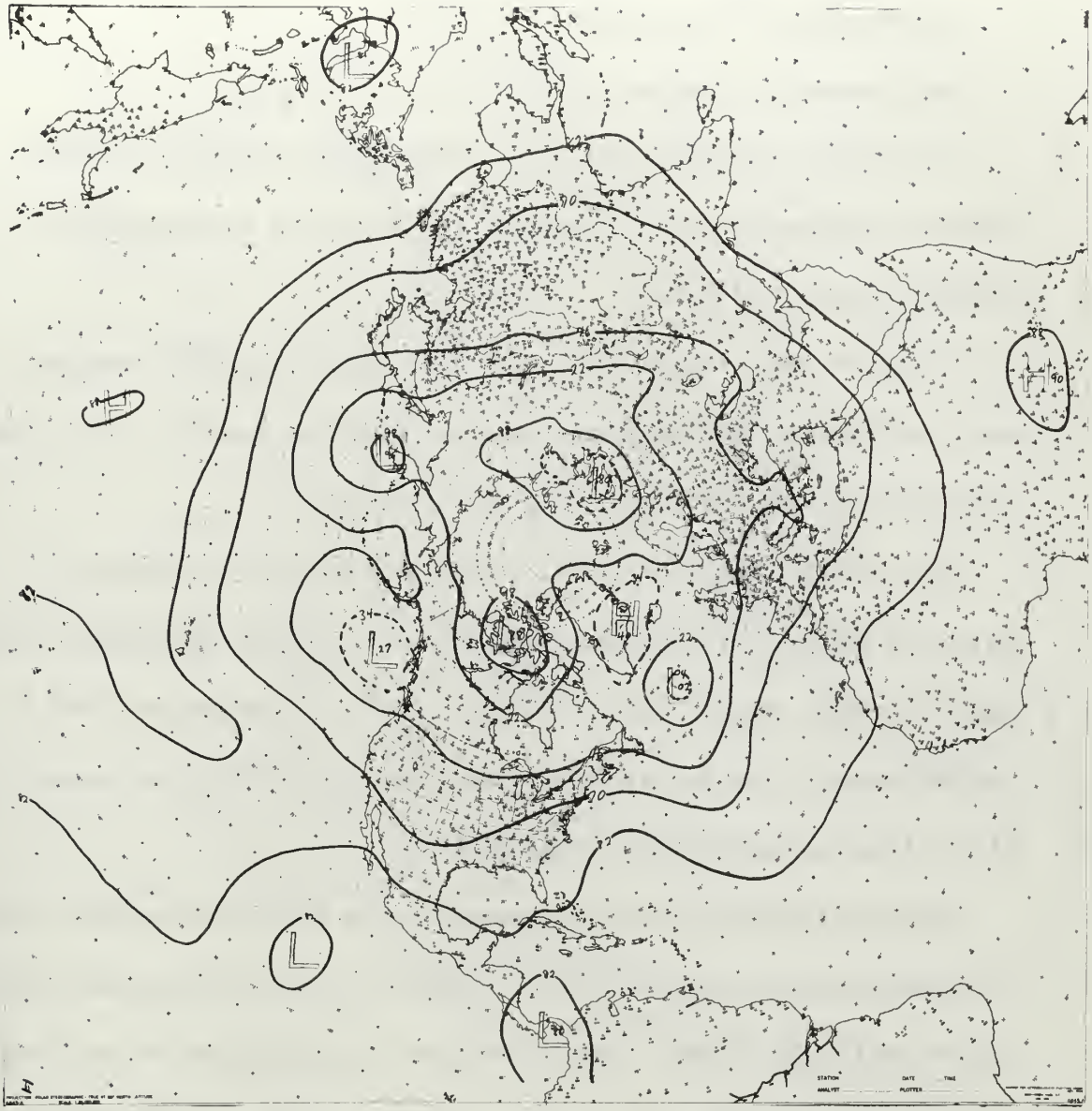


Fig. 5

For purposes of comparison, the following factors are considered:

a) the pillow(P) and RMSE(R) in feet

b) illustrative charts

c) the mean of the deviation of selected low and high central values in meters from the analysis, together with the standard deviation from this mean.

It will be seen that a low RMSE does not necessarily indicate a good verification and therefore must be carefully used in conjunction with other evidence before drawing conclusions.

For information, the FNWF pillow and RMSE for this date were 3.4 and 115.9, respectively. The mean of the deviation of lows was 7.8 with a range of 92 to -46 and a standard deviation of 47.1, and the mean of the deviation of the highs was 11.7 with a range of 31 to -2 and a standard deviation of 14.0.

Caution should be used in comparing the FNWF barotropic results to the barotropic model used here, where K_3 is 0, as this model only approximates the FNWF model. However, comparison of cases with and without the development term should indicate what effect the development term would have on the FNWF model.

The 500-mb analysis during the forecast period showed little significant movement or development with the exception of the low pressure system on the northwest coast of the U. S. which moved inland and filled, while the low in the Gulf of Alaska deepened by 90 meters and moved east leaving a trough trailing behind.

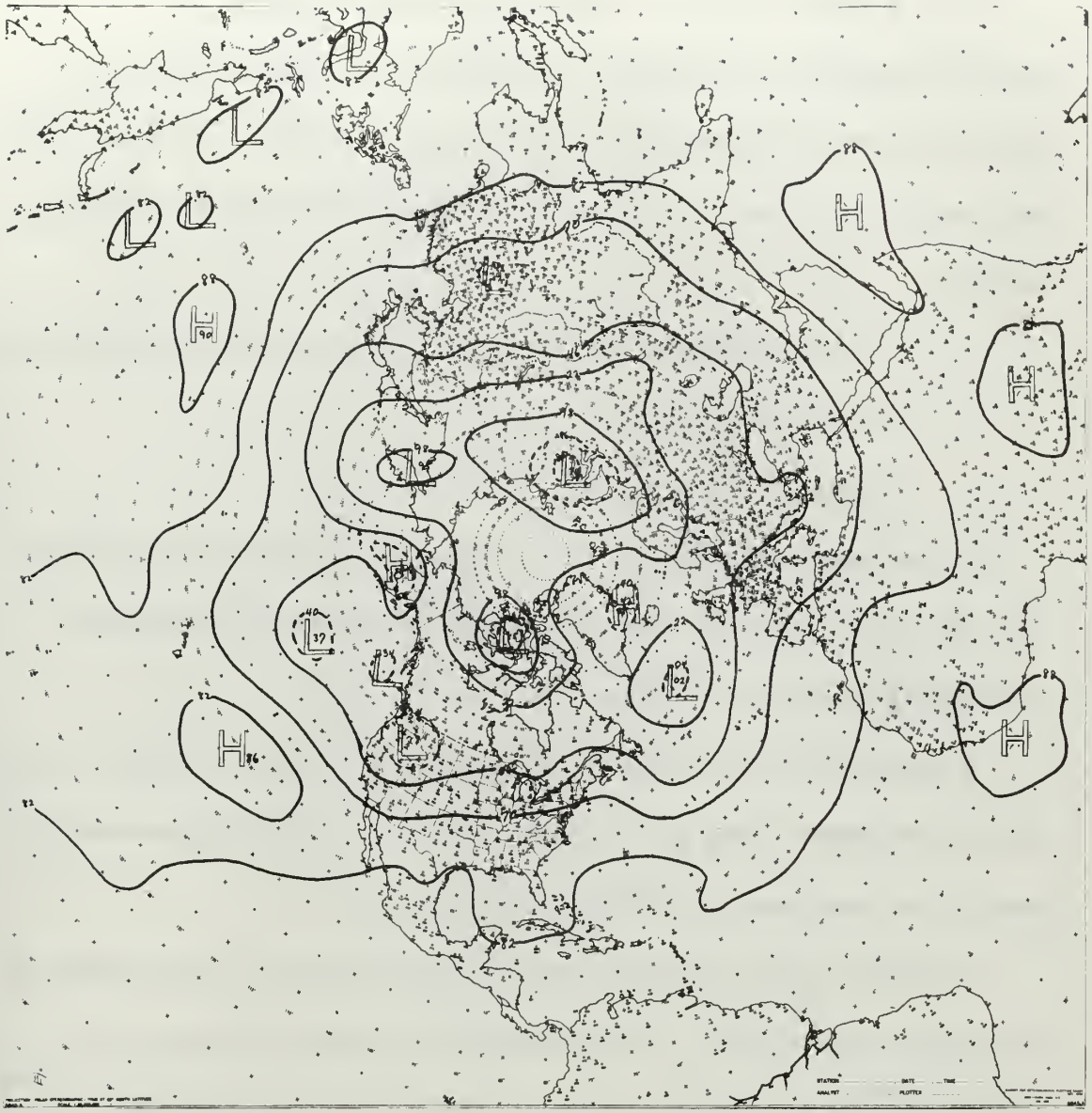


Fig. 6

Case I

Fig. 6 is the result of using no development term, $K_3 = 0$. The general position and intensity of pressure systems are good and follow the history intensities. The low on the west coast of the U. S. fails to fill while the low in the Gulf of Alaska deepens by only 20 meters.

		mean deviation and range	standard deviation from mean
P	-7	lows -5.0(51, -38)	29.6
R	105	highs 19.2(28, 9)	6.8

K_3 was next set at 1.0. The prognosis became more unstable with each time step and after 13 hours, the FNWF Helmholtz sub routine [1] would not converge.

Various other values of K_3 were tried. It was found that when K_3 is 0.5, the model runs for 18 hours, K_3 at 0.3 for 23 hours and K_3 equal to or less than 0.2, over 24 hours.

Since the hourly change of the thickness field is based solely on horizontal advection, it is believed that this field becomes less representative of the actual field fairly soon and is probably a major source of observed instability. For this reason, K_3 was divided by 2 every six hours in the following examples unless otherwise indicated. Other periodic reductions of K_3 were tried, however, this one gave the best results.

In addition, the FNWF subroutine SAU [1] is employed on the D and H fields every three hours to suppress the generation of short waves.

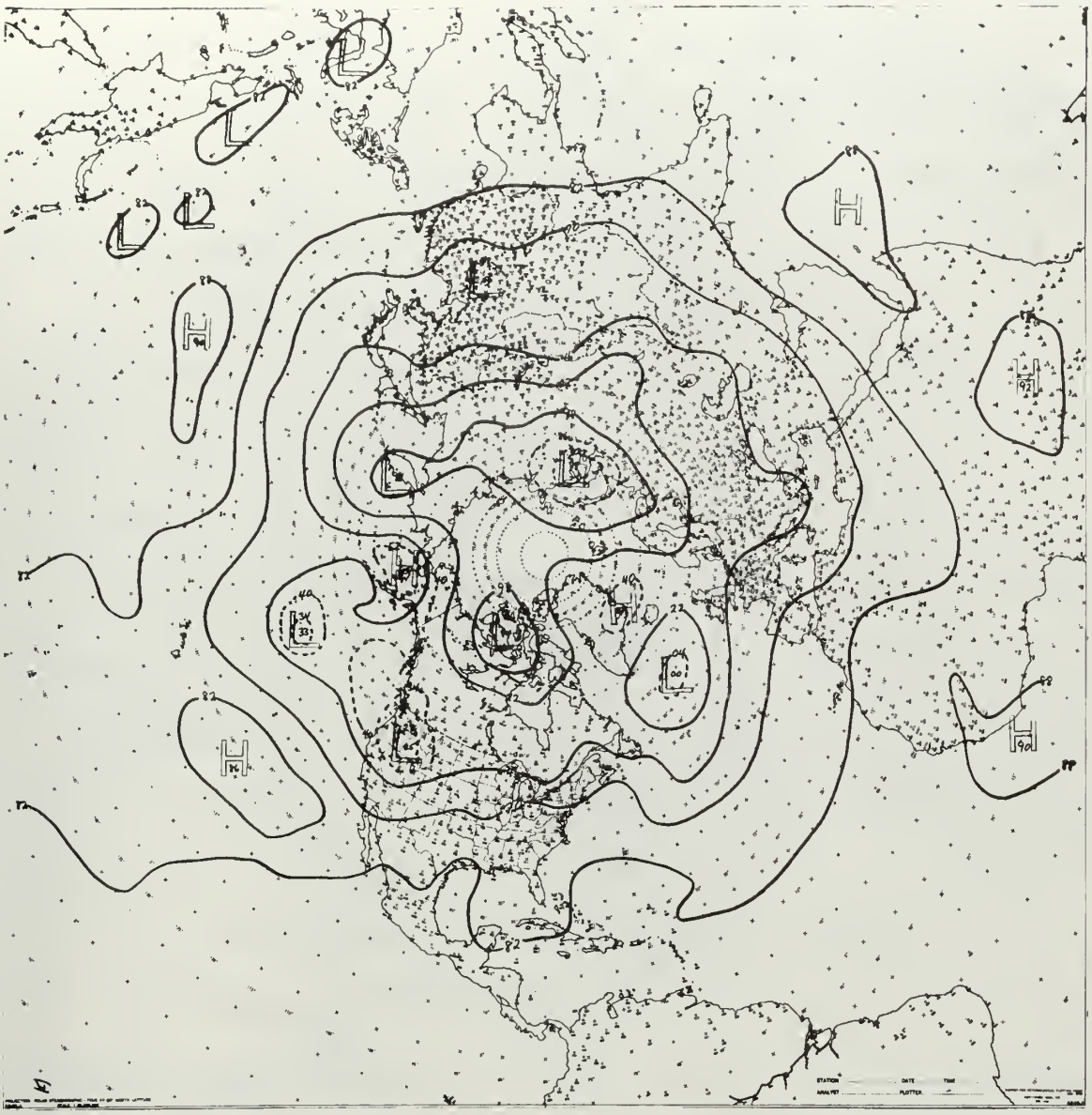


Fig. 7

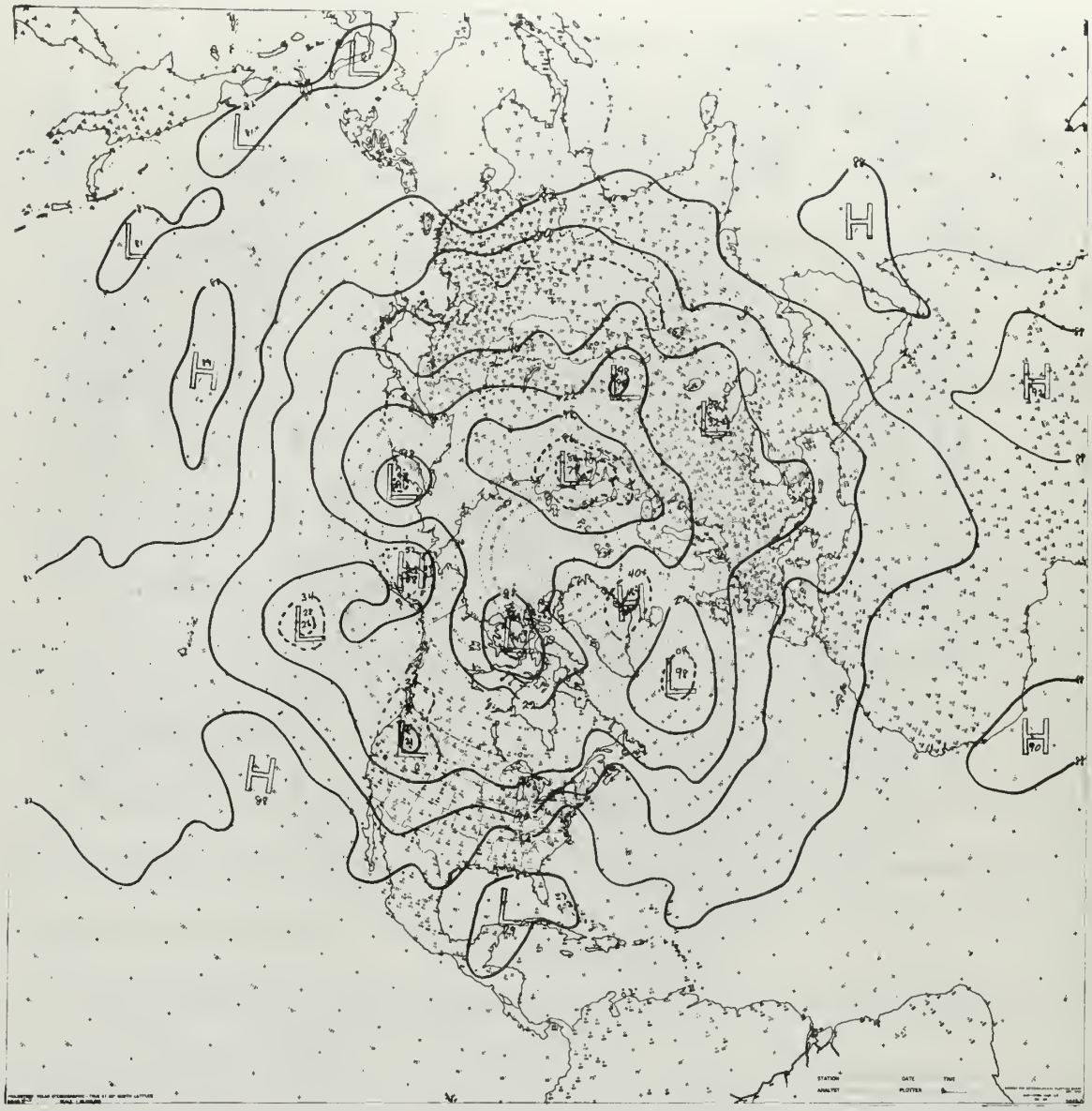


Fig. 8

Case II

In Fig. 7, K_3 is 0.5. Although the major features remain unchanged, compared to Fig. 6, there is some increase in short wave development. The mid-latitude lows are from 20 to 40 m deeper and highs 10 to 30 m higher.

			mean deviation and range	standard deviation
P	-8	lows	-8.3(45, -39)	22.7
R	115	highs	26.4(50, 8)	14.9

Case III

In Fig. 8, K_3 is increased to 1.0. Further short-wave development is noticed in addition to stronger development of both highs and lows.

The development is selective, as can be seen by the low north of Siberia remaining unchanged while the low in Idaho deepens by 50 m and the one in the Gulf of Alaska by 80 m.

			mean deviation and range	standard deviation
P	-8	lows	-16.8 (2, -43)	15.7
R	128	highs	34.6(62, 8)	22.3

In the above examples, it becomes evident that the use of the development term produces an unacceptable amount of short-wave development. FNWF has a subroutine, SAG [1] , which can be used to remove some or all perturbations. It is of the form

$$A = A + k \nabla^2 A$$

The problem remains as to what size to make k and how many times to use the smoother.

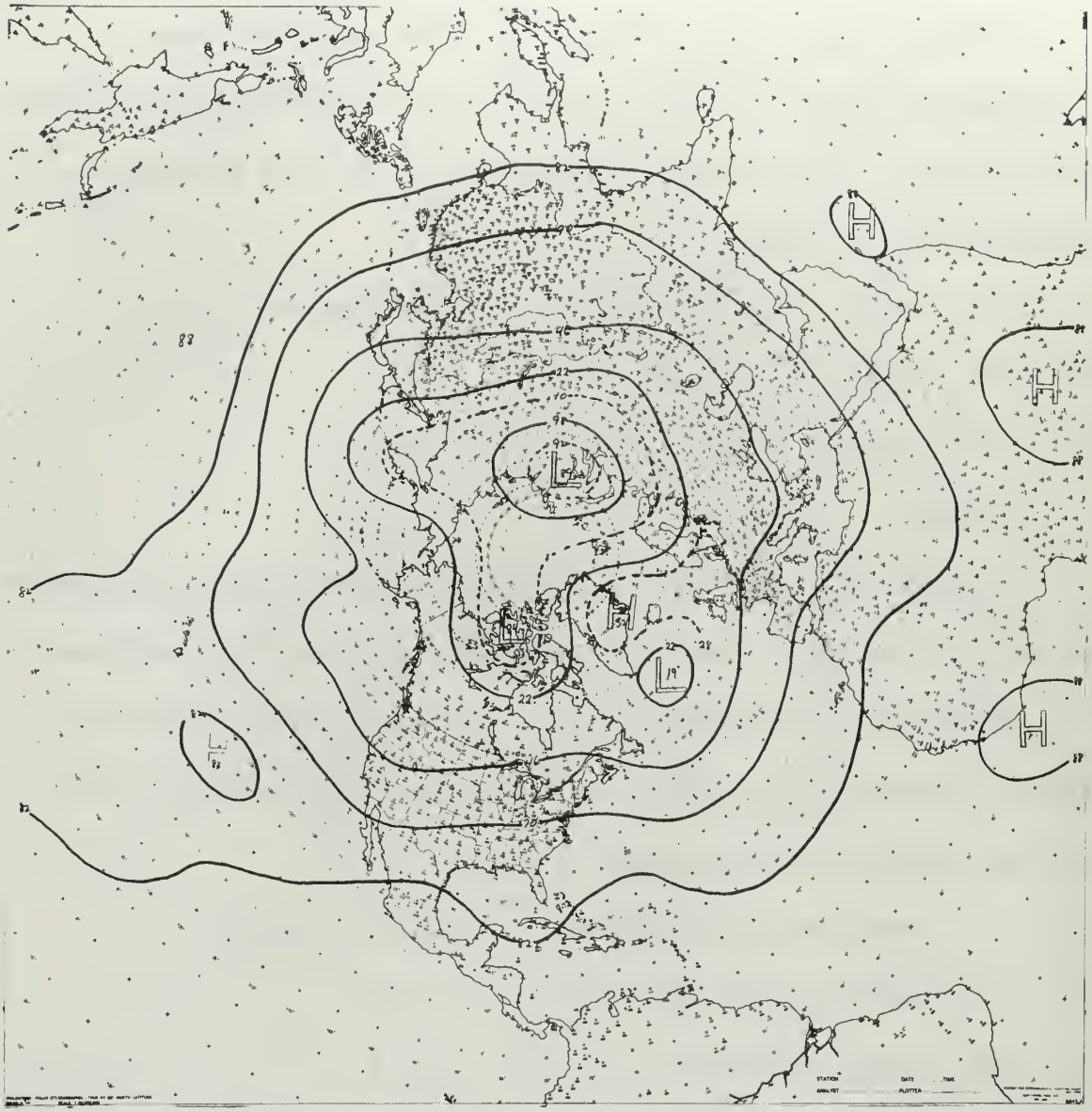


Fig. 9

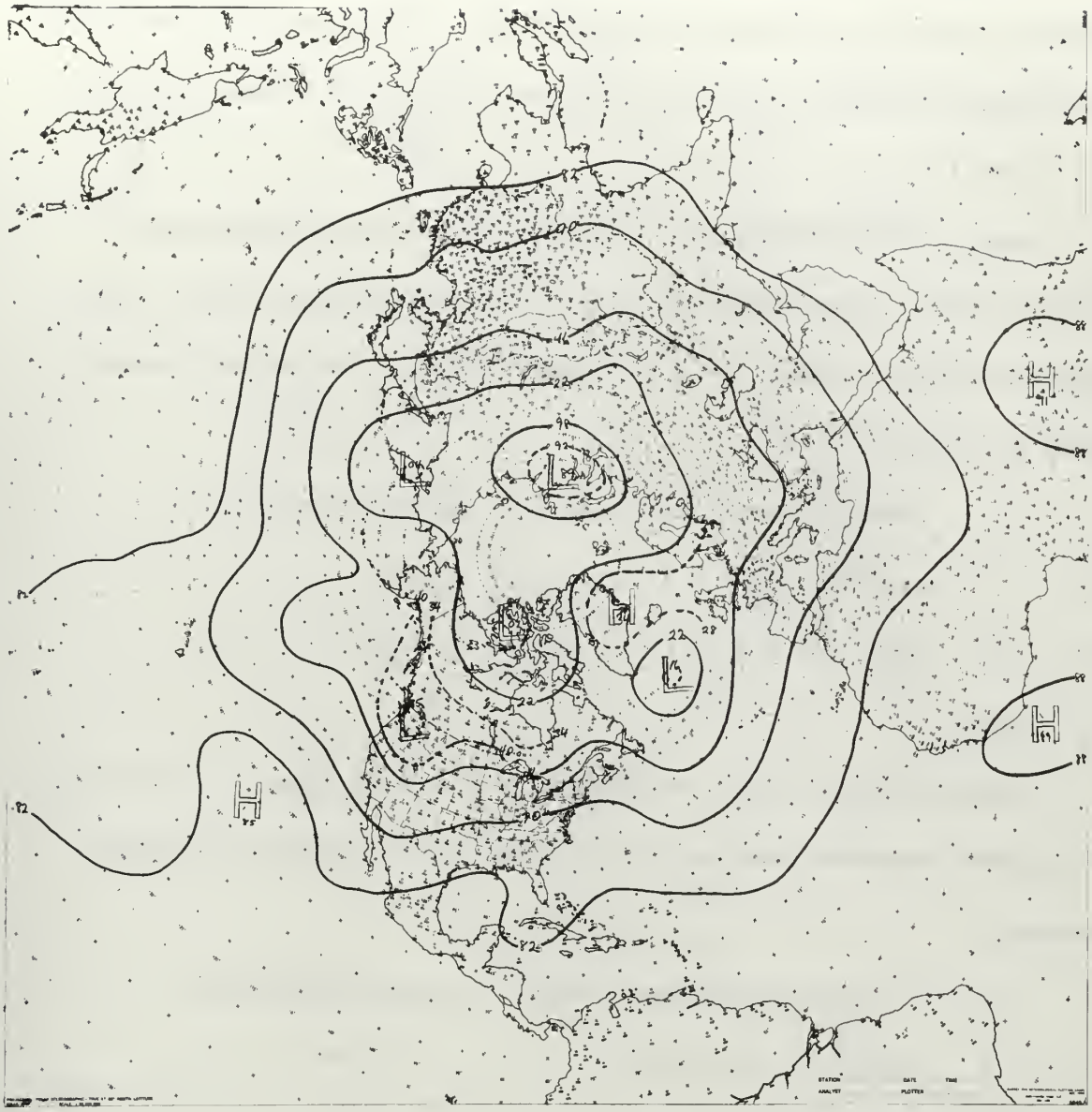


Fig. 10

The smoother was tried with k = 0.125 and used three successive times on the D and H fields every six hours. The results of this heavy smoothing in addition to no sine function and K_3 at 0 is seen in Fig. 9.

Case IV

Many of the systems have been smoothed out of existence and others have become unrepresentative of the verifying analysis. This example clearly shows that a low RMSE does not necessarily mean a good prognosis.

		mean deviation and range	standard deviation
P	-7	lows 116.0(174, 92)	32.1
R	105	highs -29.6(5, -77)	34.2

Case V

Maintaining the heavy smoothing, and setting K_3 at 1.0, starts to bring the prognosis pattern, Fig. 10, back to the analysis, but not enough.

		mean deviation and range	standard deviation
P	-8	lows 110.3(142, 84)	22.4
R	107	highs -26.2(3, -60)	32.0

Case VI

In Fig. 11, K_3 is 1.0 but is not diminished during the 24 hour period. As noted earlier, this would be too unstable to be computed, were it not for the use of a heavy smoother.

Compared to Fig. 9, both highs and lows show much greater development, but this is attained with an excessive gain in short waves.

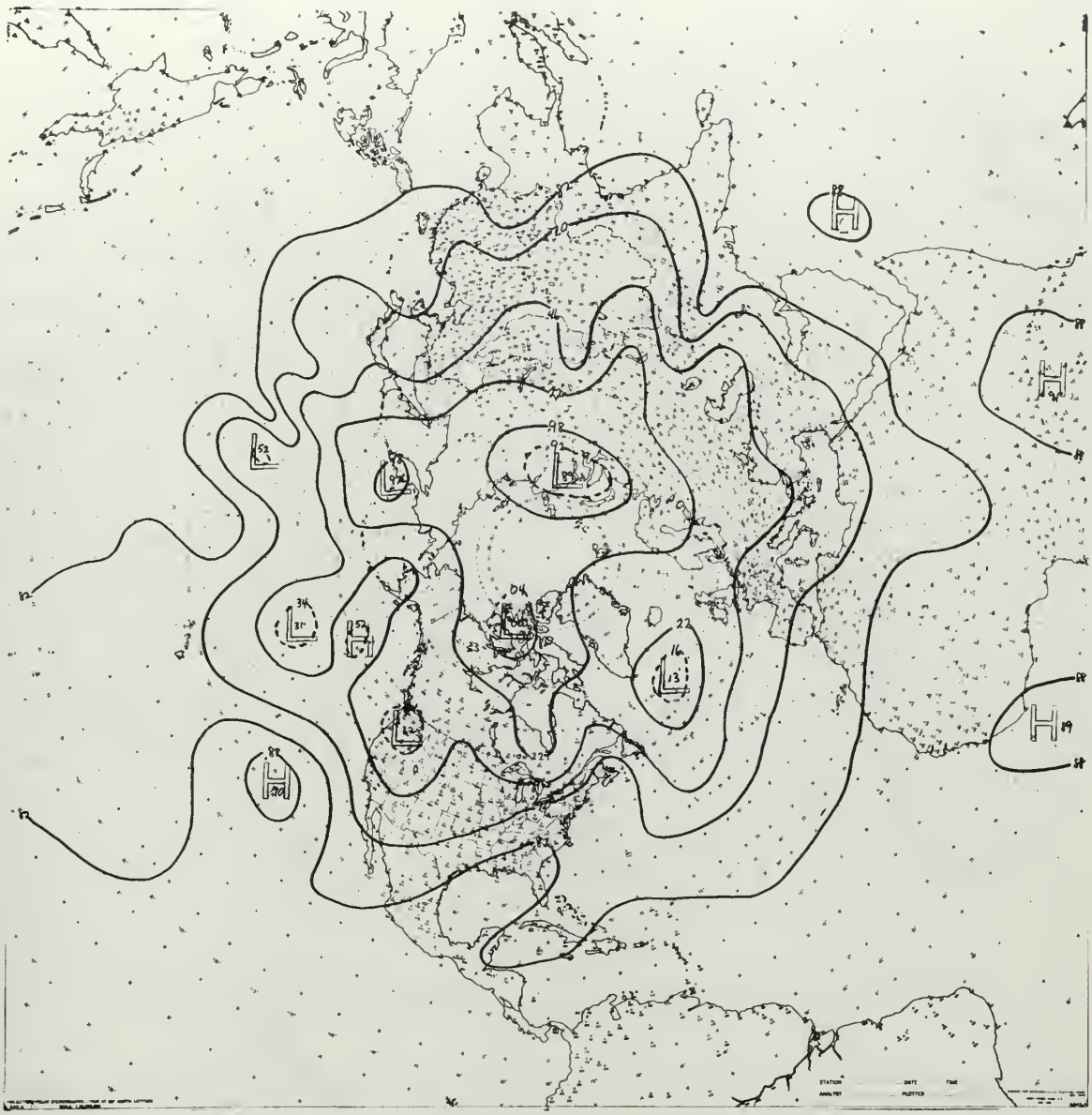


Fig. 11

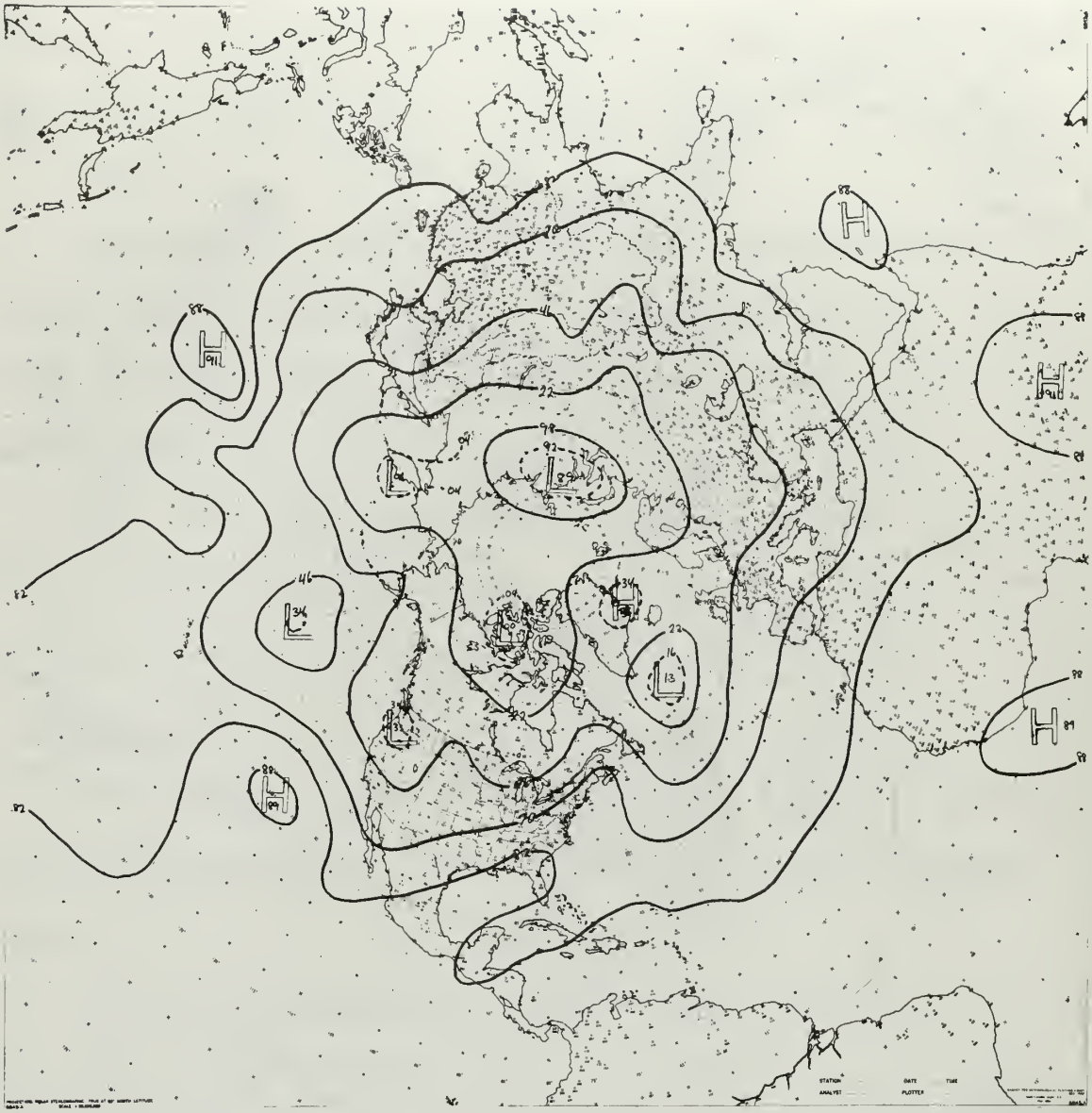


Fig. 12

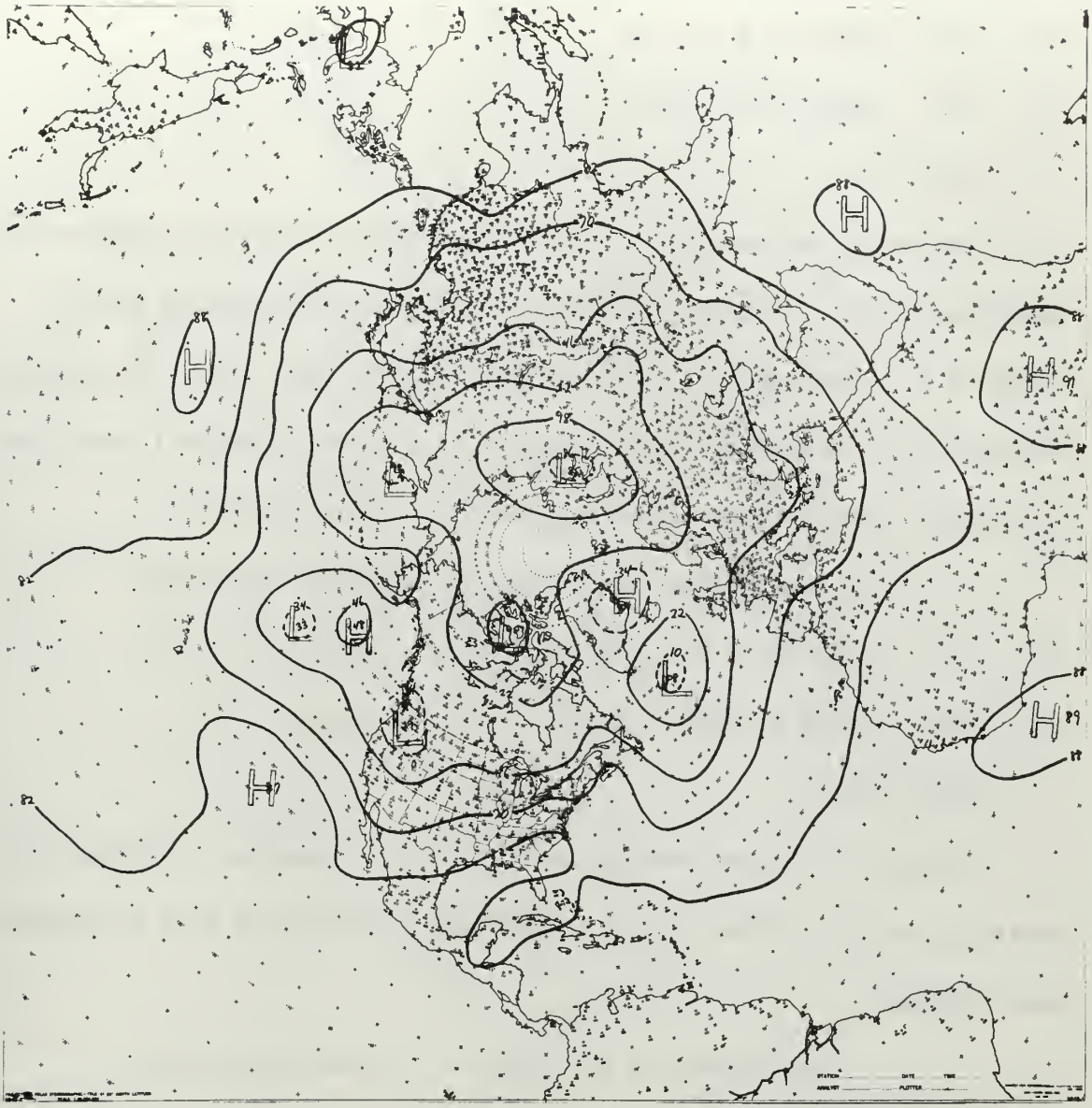


Fig. 13

		mean deviation and range	standard deviation
P	-8	lows 70.9(117, 14)	41.2
R	147	highs 8.4(63, -30)	30.5

Case VII

Continuing the search for a compromise between development and smoothness, K_3 is again divided by 2 every 6 hours and the initial value of K_3 is set at 2.0, which results in Fig. 12. While the central heights are closer to the analysis than Fig. 9 or 10, there is still too much short-wave development, although less than Fig. 11.

		mean deviation and range	standard deviation
P	-8	lows 85.5 (117, 55)	23.9
R	128	highs 6.2(53, -38)	33.0

Case VIII

In Fig. 13, the smoothing coefficient is reduced to 1/16 vice 1/8 while K_3 is 1.0. This is seen to produce development with acceptable smoothness.

		mean deviation and range	standard deviation
P	-8	lows 48.9(69, 28)	14.7
R	116	highs 4.0 (36, -21)	18.8

Case IX

Continuing in the same vein, the smoothing coefficient is reduced to 1/32 while K_3 remained 1.0, Fig. 14. Further development is noted but so is considerable short-wave formation. The compromise point has been passed.

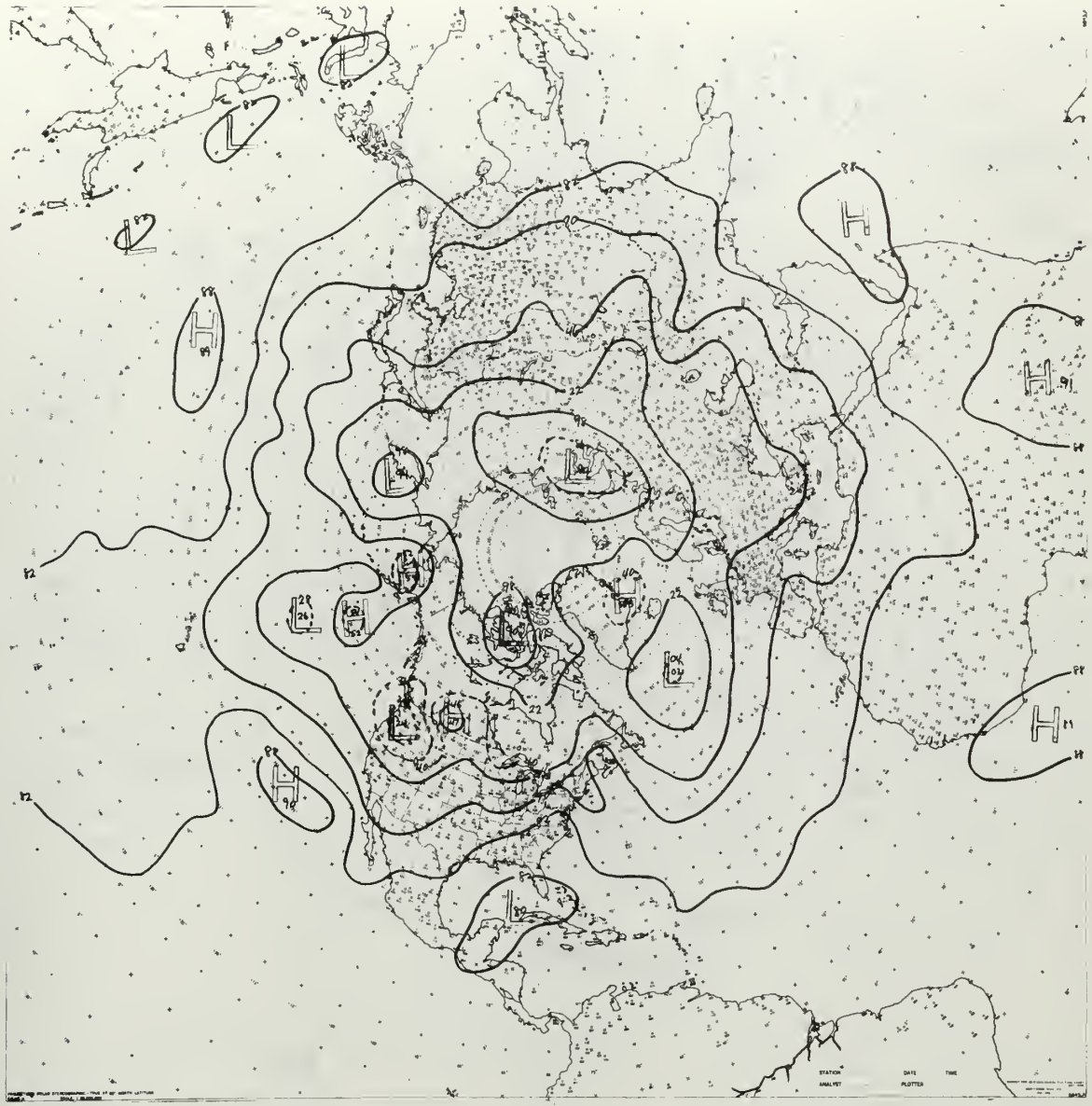


Fig. 14

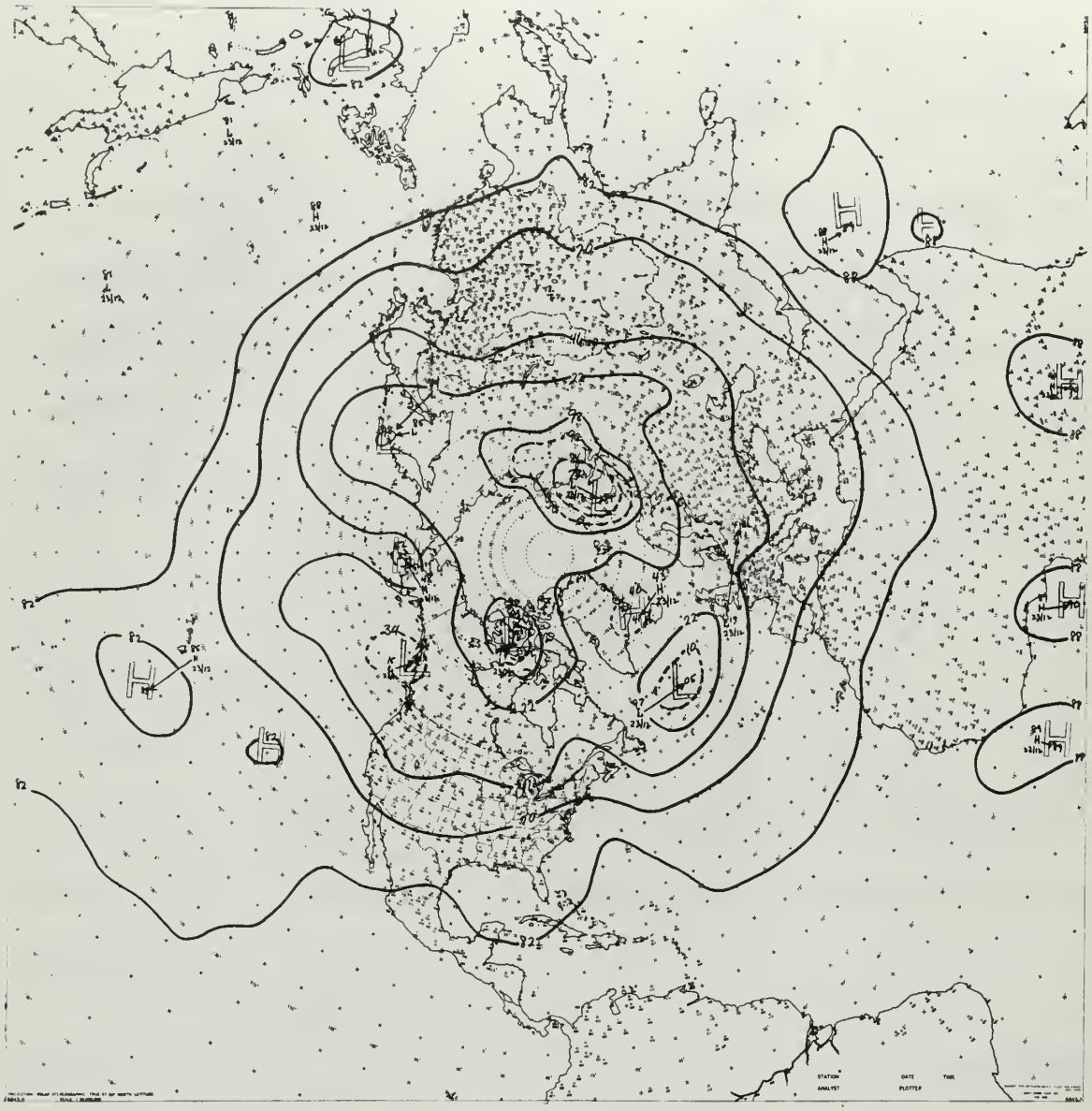


Fig. 15

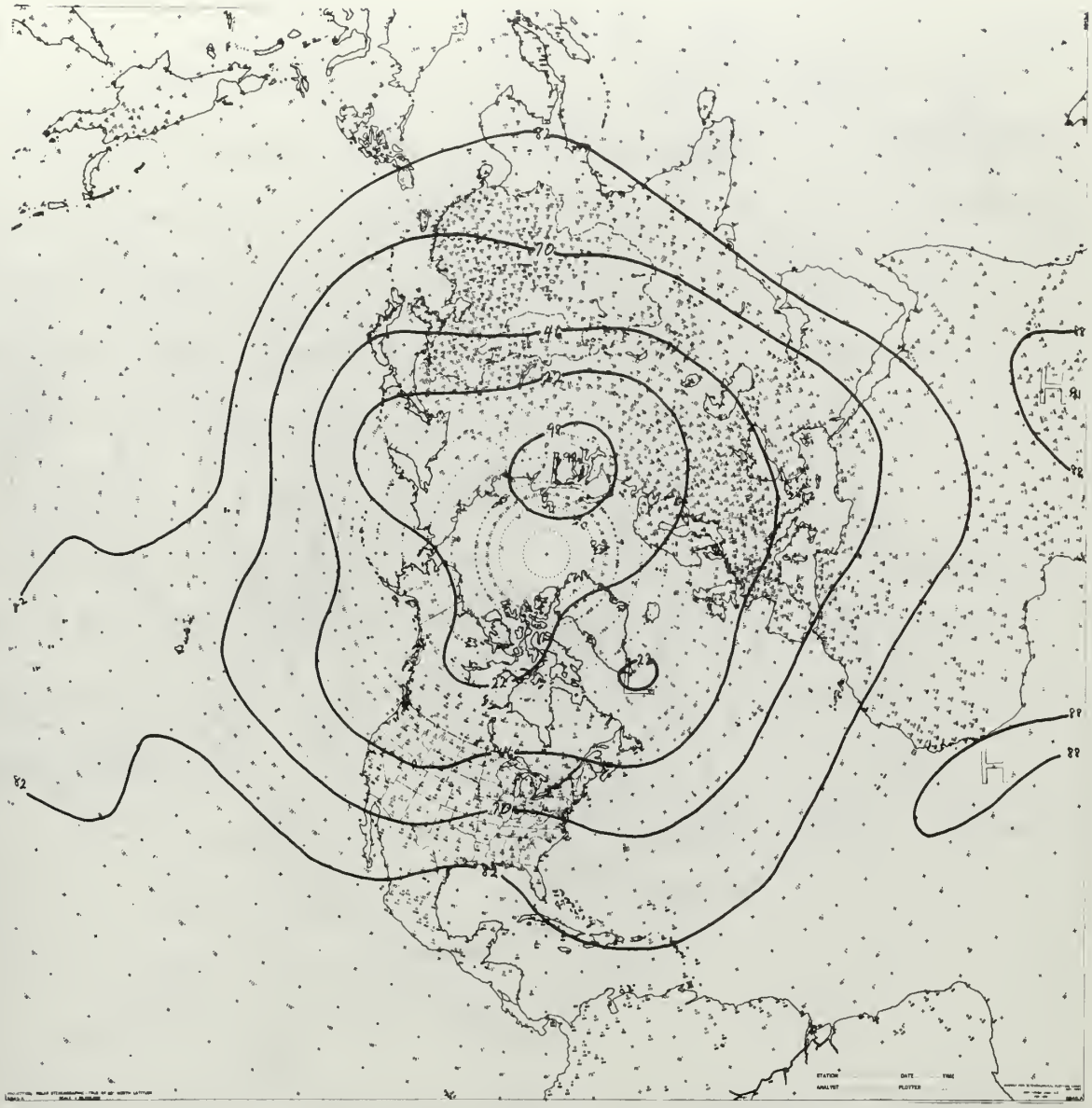


Fig. 16

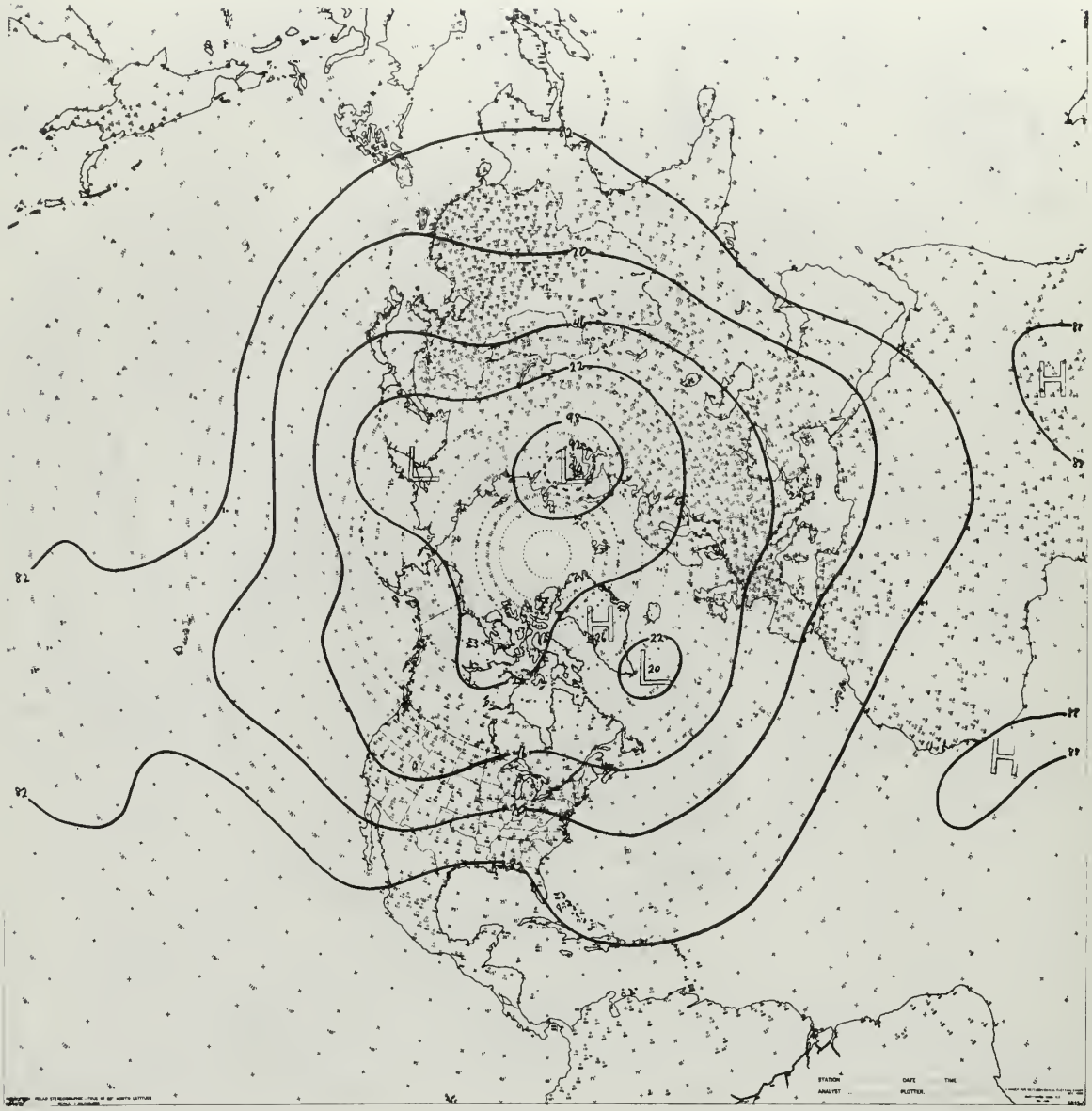


Fig. 17

		mean deviation and range	standard deviation
P	-8	lows .3(26, -22)	17.5
R	140	highs 27.6(65, 7)	21.6

The above findings are now tested for a 48 hour period using a verification analysis of 1200Z 25 Jan. 1967, Fig. 15. The FNWF pillow and RMSE for this date were -16.0 and 173.2, respectively. The mean deviation, range and standard deviation of the lows were -81.0(119, -230), 119 and for the highs -24.3(-10, -39) and 11.8.

Case X

Starting with the heavy smoother: k of 1/8, 3 scans every 6 hours, and K_3 at 0, results in Fig. 16. This is an extremely smooth chart with most baroclinic features missing. A misleading low RMSE is again encountered.

		mean deviation and range	standard deviation
P	8	lows 117.0(165, 81)	102.7
R	143	highs -154(1 sample)	-

Case XI

Continuing with the heavy smoother and changing K_3 to 1.0 produces some slight development, Fig. 17, but still far short of the analysis.

		mean deviation and range	standard deviation
P	7	lows 101.3(147, 66)	108.4
R	142	highs -154(1 sample)	-

Case XII

Reducing the smoothing factor to 1/16 with K_3 of 0 improves the chart, Fig. 18, over the previous two results but still not enough.

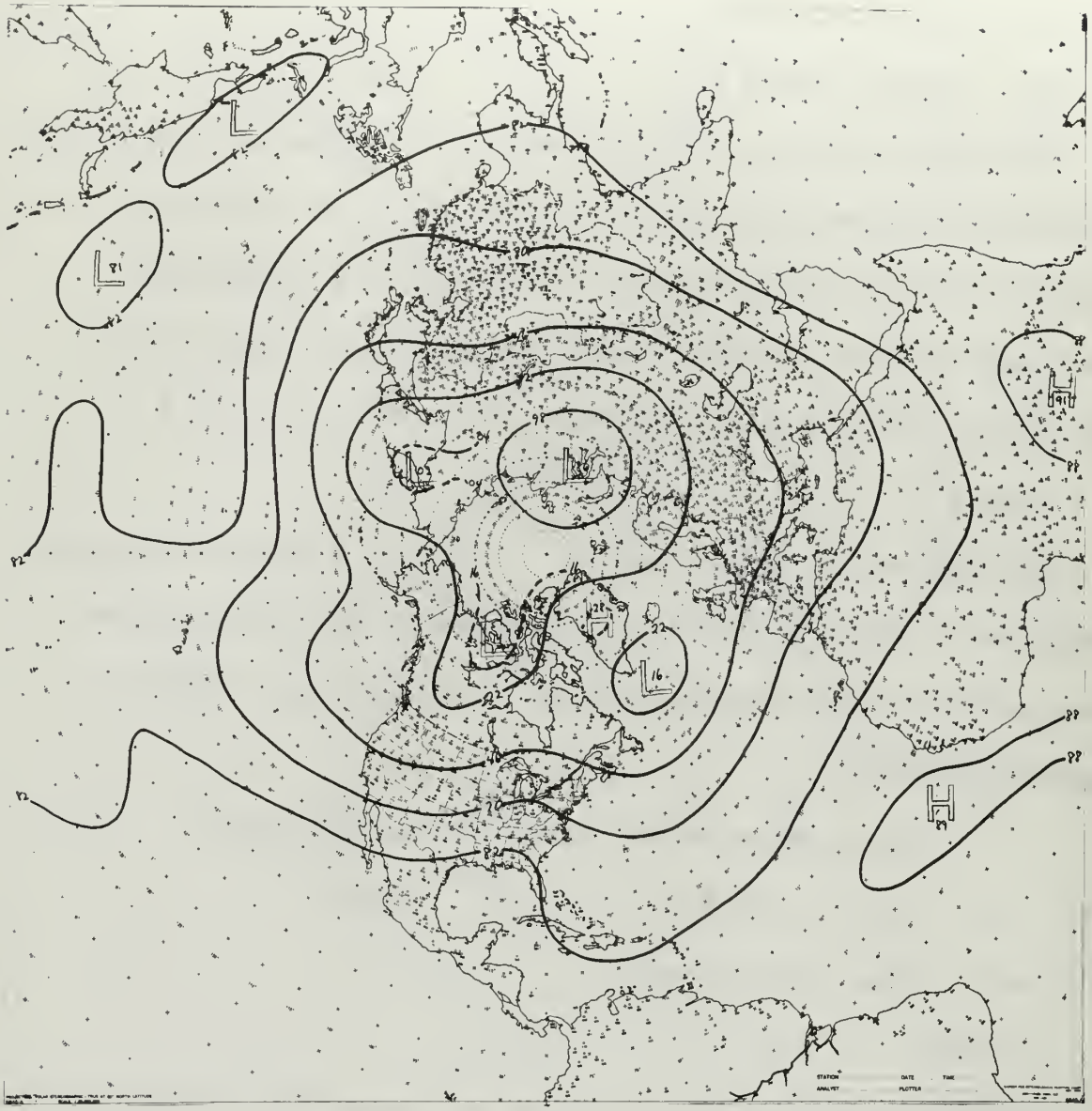


Fig. 18

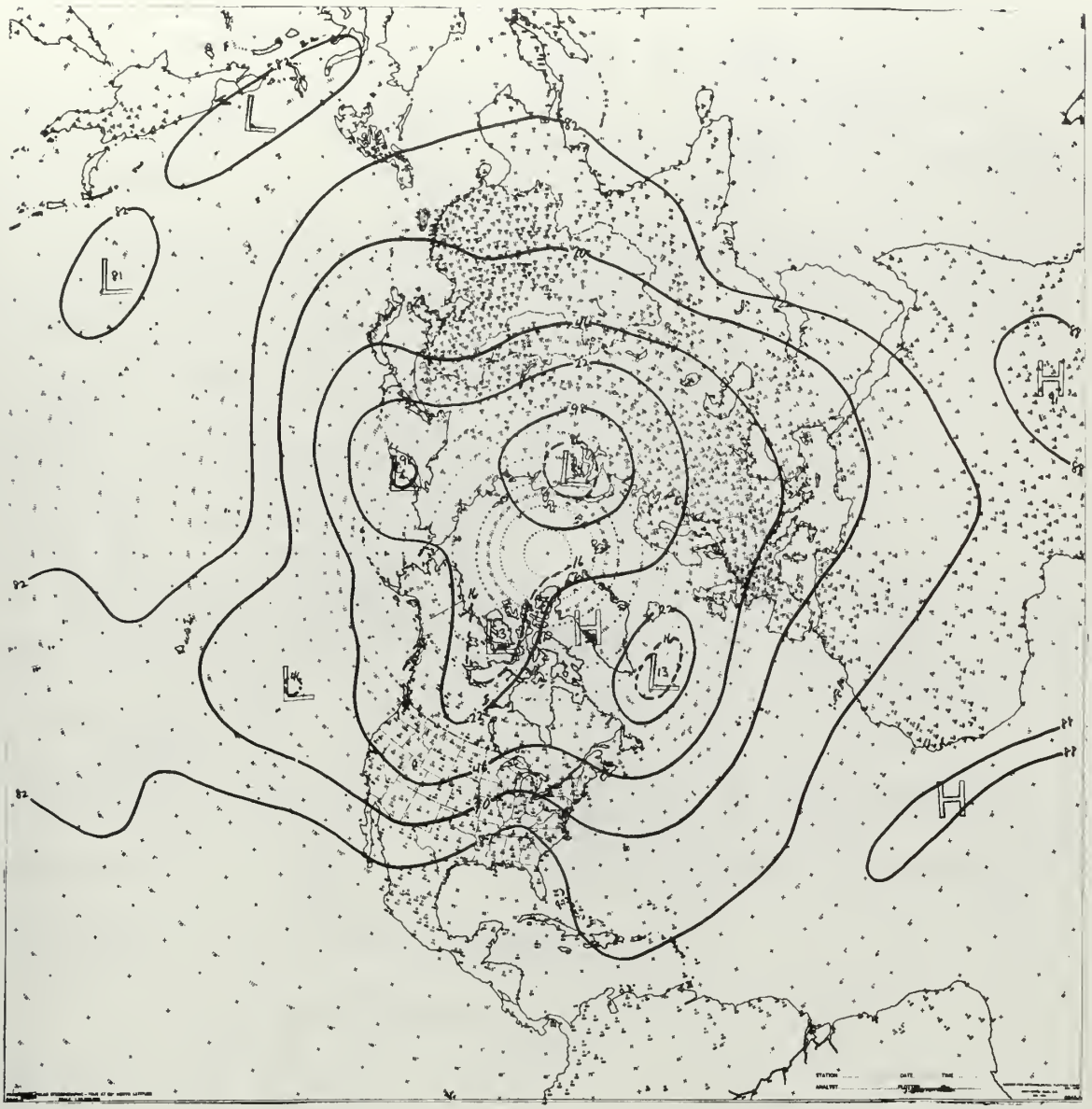


Fig. 19

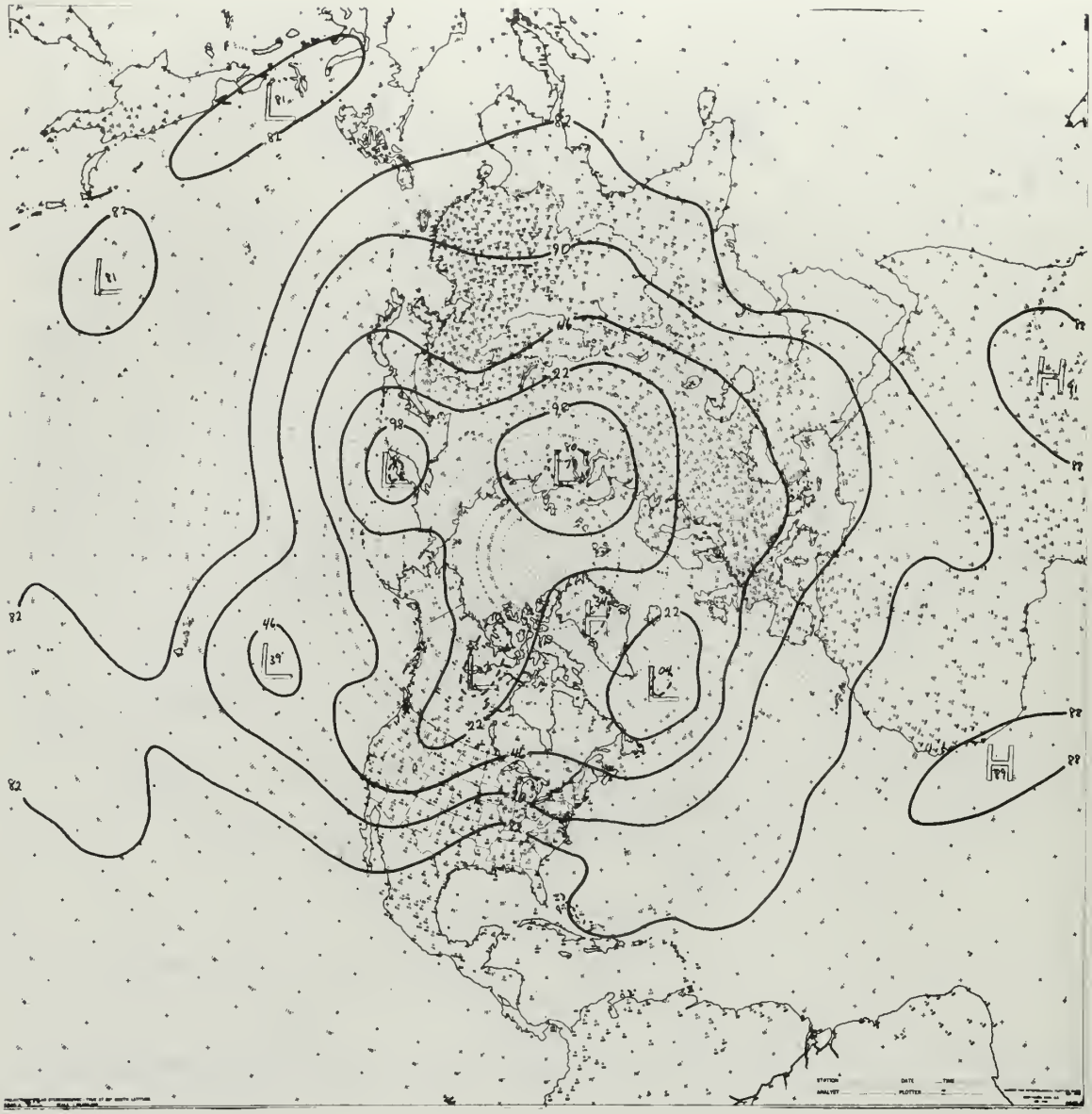


Fig. 20

		mean deviation and range	standard deviations
P	7	lows 67.0(112, 37)	110.8
R	148	highs -126(1 sample)	-

Case XIII

With the smoothing coefficient at 1/16 and K_3 at 1.0, further development is observed in Fig. 19, but even more would be desirable.

		mean deviation and range	standard deviation
P	7	lows 35.4(84, -5)	119
R	161	highs -67.0(-24, -110)	43

An attempt was made at reducing k to 1/32 while leaving K_3 at 1.0. This variation produced a 30 hour prognosis before overflow occurred.

Case XIV

The final variation, Fig. 20, was the most satisfactory although not spectacular. In this variation, k is 1/16 but used twice instead of three times every six hours while K_3 is 1.0.

		mean deviation and range	standard deviation
P	8	lows -55.4(-14, -123)	136.5
R	168	highs 5.0(62, -62)	52.4

The results of the above cases are summarized in Table III.

TABLE III

RESULTS OF VARIED DEVELOPMENT TERM VICE SMOOTHING

	Condition	P	RMSE	Mean deviation from analysis	Range	Standard deviation from mean
1.	FNWF 24 hr VT 00Z 26 Jan	3.4	115.9	Lows 7.8 Highs 11.7	92, -46 31, -2	47.1 14.0
2.	Case I	-7	105	Lows -5.0 Highs 19.2	51, -38 28, 9	29.6 6.8
3.	Case II	-8	115	Lows -8.3 Highs 26.4	45, -39 50, 8	22.7 14.9
4.	Case III	-8	128	Lows -16.8 Highs 34.6	2, -43 62, 8	15.7 22.3
5.	Case IV	-7	105	Lows 116.0 Highs -29.6	174, 92 5, -77	32.1 34.2
6.	Case V	-8	107	Lows 110.3 Highs -26.2	142, 84 3, -60	22.4 32.0
7.	Case VI	-8	147	Lows 70.9 Highs 8.4	117, 14 63, -30	41.2 30.5
8.	Case VII	-8	128	Lows 85.5 Highs 6.2	117, 55 53, -38	23.9 33.0
9.	Case VIII	-8	116	Lows 48.9 Highs 4.0	69, 28 36, -21	14.7 18.8

TABLE III (Continued)

10.	Case IX	-8	140	Lows .3 Highs 27.6	(26, -22) (65, 7)	17.5 21.6
11.	FNWF 48 hr VT 12Z 25 Jan	-16.0	173.2	Lows -81.0 Highs -24.3	119, -230 -10, -39	119.0 11.8
12.	Case X	8	143	Lows 117.0 Highs 154	313, 81 1 sample	102.7 -
13.	Case XI	7	142	Lows 101.3 Highs -154	310, 66 1 sample	108.4 -
14.	Case XII	7	148	Lows 67.0 Highs -126.0	279, 37 1 sample	110.8 -
15.	Case XIII	7	161	Lows 35.4 Highs -67.0	266, -5 -24, -110	119 43
16.	Case XIV	8	168	Lows -55.4 Highs 5.0	207, -123 62, -62	136.5 52.4

7. Independent data results

The last combination of factors, that is, K_3 of 1.0 reduced by one half every six hours and a smoothing coefficient of 1/16 applied to the height and thickness fields every six hours, was applied to independent data of seven consecutive 24-hour prognostic charts.

These charts covered the period 0000Z 24 March to 0000Z 27 March. A comparison was made with full development term of 1.0, no development term and the FNWF product for these dates.

Upon summarizing the results of the above tests, it was seen that a K_3 of 1.0 was probably too high and another group of seven charts was produced with a K_3 of 0.7.

The results of all of the above are listed in Table IV. The pillow and RMSE for the variations on the applicable dates is presented in Table V.

Table IV indicates a sharp reduction in the mean deviation of the lows from the analysis, however, the choice of a K_3 of 0.7 was too much of a reduction from 1.0 in the case of the lows but was quite good for the highs. A K_3 of about 0.8 would probably have produced better results for this period.

Compared to FNWF, a K_3 of 0.7 results in a good reduction in the range of deviations for both highs and lows and a marked improvement for the standard deviation from the mean deviation for highs.

TABLE IV

INDEPENDENT DATA TEST OF DEVELOPMENT TERM

	LOWS (31 cases)			HIGHS (12 cases)		
	Mean deviation from analysis	Range	Standard deviation	Mean deviation from analysis	Range	Standard deviation
K3=0	+49.9	(+147, -5)	39.6	-9.1	(+28, -46)	16.6
K3=1	-2.2	(+82, -50)	40.9	+8.2	(+79, -30)	27.3
FNWF	2.9	(+106, -70)	42.0	-5.6	(+70, -75)	42.5
K3=.7	+18.1	(99, -30)	40.2	+1.3	(62, -38)	23.4

TABLE V

INDEPENDENT DATA TEST OF DEVELOPMENT TERM
PILLOW AND RMSE (ft.)

V.T.	K3=0	K3=1.0	K3=.7	FNWF
0000Z 24 Mar	P -1	-2	-2	1.1
	R 93	96	92	104
1200Z 24 Mar	P -5	-5	-5	6.3
	R 101	106	100	115.3
0000Z 25 Mar	P -5	-5	-5	6.6
	R 90	101	92	108.3
1200Z 25 Mar	P 5	5	5	-3.8
	R 97	101	95	105.9
0000Z 26 Mar	P 0	0	0	-.3
	R 113	113	109	111.1
1200Z 26 Mar	P -2	-2	-2	-1.2
	R 117	119	115	115.0
0000Z 27 Mar	P 18	17	17	-25.5
	R 94	101	95	101.5

8. Conclusions

The modification of the horizontal advection term by a function of latitude as used herein, generally improved the movement of troughs and ridges by reducing the lag between prognosis and analysis.

It appears that a refinement of this function with a displacement of the maximum from about 20 degrees to about 45 degrees would be more rewarding.

While compiling data for this study, there appeared to be a relation between the zonal index and the lag of the troughs and ridges. It is recommended that further study of this phenomena be conducted to arrive at a more exact relationship and how it could be applied to proper movement of troughs and ridges.

It is readily seen that, as the name implies, the development term produces development in the form of deeper lows, higher highs and also, unfortunately, unwanted short waves.

It results in distinct and selective changes in intensities of systems without materially changing the location of these systems.

It showed marked improvement over the FNWF highs and a lowering of the range of errors in the lows.

The inclusion of this term to some degree in an operational barotropic model would be beneficial.

It is suggested that the most desirable approach would be to incorporate these empirical modifications in the FNWF 500-mb prediction equation while simultaneously carrying out the FNWF 1000-mb prediction hour by hour. The resulting H field could then be incorpor-

ated into the 500-mb forecasts each hour, which should be far more reliable than that produced by simple advection of thickness.

A development term so produced could be made smaller initially, say $K_3 = 0.25$, but would not be reduced periodically since the thickness field would presumably stay in phase better with the 500-mb height field.

This scheme should produce improved long range 500-mb and surface prognostic charts.

9. Acknowledgments

My gratitude is extended to Professor G. J. Haltiner for planting the seed of this interesting project and the helpful, patient staff of FNWF, in particular Mr. L. C. Clarke, and LT P. G. Kesel.

BIBLIOGRAPHY

1) FNWF handbook of scrap subroutines. Unpublished, 1964.

2) Haltiner, George J., and Frank L. Martin. Dynamical and Physical Meteorology. McGraw-Hill Book Company, Inc., 1957.

3) Hughes, R. E. "Computer Products Manual", Technical Note No. 21. Fleet Numerical Weather Facility, July 1966.

4) Thompson, P. D. Numerical Weather Analysis and Prediction. MacMillan Company, 1961.

INITIAL DISTRIBUTION LIST

		No. Copies
1.	LCDR Howard L. Lewit, USN Headquarters, Pacific Missile Range Box 22, Code 3250 Point Mugu, California 93041	1
2.	Professor G. J. Haltiner Department of Meteorology & Oceanography Naval Postgraduate School Monterey, California 93940	3
3.	Library Naval Postgraduate School Monterey, California 93940	2
4.	Department of Meteorology & Oceanography Naval Postgraduate School Monterey, California 93940	1
5.	Defense Documentation Center Cameron Station Alexandria, Virginia 22314	20
6.	Office of the Naval Weather Service Naval Station (Washington Navy Yard Annex) Washington, D. C. 20390	1
7.	Officer in Charge Fleet Numerical Weather Facility Naval Postgraduate School Monterey, California 93940	2
8.	Commanding Officer FWC/JTWC Box 12, COMNAVMARIANAS FPO San Francisco 96601	1
9.	Commanding Officer U. S. Fleet Weather Central FPO Seattle 98790	1
10.	Commanding Officer U. S. Fleet Weather Central Box 110 FPO San Francisco 96610	1

11. Commanding Officer — 1
U. S. Fleet Weather Central
Box 31
FPO New York 09540

12. Commanding Officer — 1
Fleet Weather Central
Navy Department
Washington, D. C. 20390

13. Commanding Officer — 1
Fleet Weather Central
Naval Air Station
Alameda, California 94501

14. Officer in Charge — 1
U. S. Fleet Weather Facility
FPO New York 09597

15. Officer in Charge — 1
U. S. Fleet Weather Facility
FPO New York 09510

16. Officer in Charge — 1
U. S. Fleet Weather Facility
FPO New York 09571

17. Officer in Charge — 1
U. S. Fleet Weather Facility
FPO San Francisco 96662

18. Officer in Charge — 1
U. S. Fleet Weather Facility
FPO San Francisco 96652

19. Officer in Charge — 1
Fleet Weather Facility
Naval Air Station
San Diego, California 92135

20. Officer in Charge — 1
Fleet Weather Facility
Naval Air Station
Norfolk, Virginia 23511

21. Officer in Charge — 1
Fleet Weather Facility
Naval Air Station
Quonset Point, Rhode Island 02819

22. Officer in Charge — 1
Fleet Weather Facility
Box 85
Naval Air Station
Jacksonville, Florida 32212

23. Officer in Charge — 4
Navy Weather Research Facility
Bldg. R-48
Naval Air Station
Norfolk, Virginia 23511

DOCUMENT CONTROL DATA - R&D

(Security classification of title, body of abstract and indexing annotation must be entered when the overall report is classified)

1. ORIGINATING ACTIVITY (Corporate author)
Naval Postgraduate School
Monterey, California 93940

2a. REPORT SECURITY CLASSIFICATION
Unclassified

2b. GROUP

3. REPORT TITLE
THE EXPERIMENTAL MODIFICATION OF A BAROTROPIC NUMBERICAL PREDICTION MODEL

4. DESCRIPTIVE NOTES (Type of report and inclusive dates)
Thesis

5. AUTHOR(S) (Last name, first name, initial)
LEWIT, Howard L., LCDR, USN

6. REPORT DATE	7a. TOTAL NO. OF PAGES	7b. NO. OF REFS
June 1967	62	4

8a. CONTRACT OR GRANT NO.	9a. ORIGINATOR'S REPORT NUMBER(S)
b. PROJECT NO.	
c.	9b. OTHER REPORT NO(S) (Any other numbers that may be assigned this report)
d.	

10. AVAILABILITY/LIMITATION NOTICES
[redacted]

11. SUPPLEMENTARY NOTES	12. SPONSORING MILITARY ACTIVITY

13. ABSTRACT

There were two objectives in the experiments performed on the barotropic model. One was to correct the lag of the troughs and ridges noted in the barotropic model by the Naval Weather Research Facility, and the other was to introduce a baroclinic term.

The approach to these problems was one which could be incorporated into the Fleet Numerical Weather Facility model with ease.

Included herein are the theoretical development of the numerical model, a comparison with the FNWF model and charts illustrative of the results with various values of the pertinent parameters for 24 and 48 hours.

It was observed that the development term causes selective development of lows and highs; but when overdone, spurious short waves are formed which, however, do not basically change the major wave location.

It was also observed that the function of latitude used here to correct the lag in the horizontal advection of vorticity, resulted in greatly improved movement of troughs and ridges from 30 degrees to 60 degrees of latitude, but could be further refined to produce even better results.

14 KEY WORDS	LINK A		LINK B		LINK C	
	ROLE	WT	ROLE	WT	ROLE	WT
BAROTROPIC MODEL DEVELOPMENT TERM NUMERICAL PROGNOSIS						

thesL617
DUDLEY KNOX LIBRARY
3 2768 00416517 5
DUDLEY KNOX LIBRARY